universität wien

DIPLOMARBEIT / DIPLOMA THESIS

Titel der Diplomarbeit / Title of the Diploma Thesis

„Potential Cooperativity between BET inhibition and Nrf2 activation in activated vascular smooth muscle cells“

verfasst von / submitted by

Nisa Kellerlioglu

angestrebter akademischer Grad / in partial fulfilment of the requirements for the degree of

Magistra der Pharmazie (Mag.pharm.)

Wien, 2019 / Vienna, 2019

Studienkennzahl lt. Studienblatt / degree programme code as it appears on the student record sheet:	A 449
Studienrichtung lt. Studienblatt / degree programme as it appears on the student record sheet:	Diplomstudium Pharmazie
Betreut von / Supervisor:	Ass. Prof. Dr. Elke Heiß

Abstract

Cardiovascular diseases, the leading cause of death in the developed world, are mainly caused by atherosclerosis. In life-threatening cases surgical interventions, such as bypass or stents, are unavoidable, although their shortcomings are recognized due to the possible ensuing restenosis. Restenosis is associated with the proliferation of vascular smooth muscle cells (VSMC) and the migration into the tunica intima, which then again causes a decrease of arterial lumen space. Hence, inhibiting VSMC proliferation e.g. by coating stents with antimitogenic compounds could sustain the benefit of surgical interventions.

Sulforaphane, a naturally occuring isothiocyanate, is one of the compounds that shows an anti-proliferative effect on primary VSMCs. It is known for activating the Nrf2 pathway, which plays a pivotal role in the protection of cells against e.g. oxidative stress, inflammation, xenobiotics or metabolic imbalance.

Another compound reported to be anti-proliferative for VSMCs is JQ1, a BET-protein inhibitor. BET-proteins are able to 'read' the acetylation code of histones, thereby controlling gene expression. Since BET-protein inhibitors positively influence Nrf2 signaling and also lead to VSMC proliferation inhibition, the combination of Sulforaphane as an Nrf2 activator and JQ1 as a BET-protein inhibitor could lead to a stronger inhibitory effect on VSMC proliferation. The aim of this diploma thesis is therefore to investigate the effect of the single and combinatorial treatment of SFN and JQ1 on VSMC proliferation.

Initially, the half maximal inhibitory concentrations (IC50) for Sulforaphane and JQ1 in serum und PDGF stimulated VSMC were determined with the crystal violet assay. The IC50 of SFN is 5.05 µM for serum stimulated and 1.39 µM for PDGF stimulated cells. The IC50 of JQ1 lies at 889 nM for serum stimulated and 102 nM for PDGF stimulated cells.

Furthermore, the combination of Sulforaphane and JQ1 did not lead to a synergistic anti-proliferative effect in VSMCs, but rather to an antagonistic effect. The combinatorial indexes increased with higher concentrations of JQ1 both in serum and

PDGF stimulated cells.

Apart from that, the cell cycle distribution upon SFN and JQ1 treatment was investigated with flow cytometry and showed a G1 cell cycle arrest for both compounds.

By using the western blotting technique, target proteins of the NRF2 pathway, such as HO-1 and GCLC, as well as BRD4 and PDGF-R levels, which are reported to be up-regulated in activated VSMC, were quantified. The results showed a rather additive or synergistic effect of SFN and JQ1 in up-regulation of Nrf2 target genes. BRD4 and PDGFR levels were not altered much by either compound or their combination. Thus, further investigations are required to understand the molecular mechanism behind the antagonistic effect of SFN and JQ1 with regards to the inhibition of VSMC proliferation.

Zusammenfassung

Die Ursache vieler kardiovaskulärer Erkrankungen - die häufigste Todesursache in Industriestaaten - ist in den meisten Fällen die Atheriosklerose. In lebensgefährlichen Situationen sind chirurgische Eingriffe wie Bypass oder Gefäßstützen (*stent*), die jedoch aufgrund der Restenose unzureichend sind bzw. keine dauerhafte Abhilfe bringen, unumgänglich. Restenose ist bedingt von der Proliferation und Migration von glatten Gefäßmuskelzellen von der Tunica media in die Tunica intima und resultiert in einer Verengung des Gefäßlumens. Daher ist die Inhibierung der Proliferation von glatten Gefäßmuskelzellen durch den Einsatz antimitogener Substanzen und beschichteten *stents* ein wichtiger Ansatz in der Therapie der durch chirurgischen Einsatz verursachten Restenose.

Sulforaphan, ein chemopräventives Isothiocyanat aus Brassica species, zeigt einen antiproliferativen Effekt in glatten Gefäßmuskelzellen. Als ein Aktivator des Nrf2-Signalweges spielt es eine bedeutende Rolle beim Schutz der Zellen vor beispielsweise oxidativen Stress, Entzündungen, Xenobiotika und Stoffwechselentgleisungen.

Eine weitere für glatte Gefäßmuskelzellen anti-proliferativ wirkende Substanz ist JQ1, ein BET - Protein Inhibitor. BET – Proteine sind in der Lage den Acetylierungscode von Histonen zu „lesen“ und können dadurch die Genexpression beeinflussen. Da BET – Proteine zu einer Herabregulierung des Nrf2 – Signalweges führen und ebenso die Proliferation von glatten Gefäßmuskelzellen inhibieren, könnte die Kombination von Sulforaphan als Nrf2 – Aktivator und JQ1 als BET - Protein Inhibitor zu einem verstärkten inhibitorischen, anti-proliferativen Effekt in glatten Gefäßmuskelzellen führen. Daher ist das Ziel dieser Diplomarbeit den Effekt von SFN zusammen mit JQ1 in glatten Gefäßmuskelzellen zu untersuchen.

Zuerst wurden die halb maximalen inhibitorischen Konzentrationen (IC_{50}) für Sulforaphan und JQ1 in Serum und PDGF stimulierten Zellen mithilfe des Kristallviolett-assays bestimmt. Der IC_{50} Wert von Sulforaphan lag bei 5.05 µM in Serum- und bei 1.39 µM in PDGF stimulierten Zellen. Für JQ1 betrugen die IC_{50} Werte 889 nM in Serum- und 102 nM in PDGF stimulierten Zellen.

Anschließend konnte gezeigt werden, dass die Kombination beider Substanzen nicht zu einem synergistischen, anti-proliferativen Effekt in glatten Gefäßmuskelzellen geführt hat, sondern zu einem antagonistischen Effekt. Der kombinatorische Index (CI) steigt mit erhöhter Konzentration von JQ1 sowohl in Serum- als auch in PDGF stimulierten Zellen.
Des Weiteren zeigten Zellzyklusanalysen mit dem Durchflusszytometer für beide Substanzen einen G1 Zellzyklus-arrest.
Zuletzt wurden Zielgen- Proteine des Nrf2 Signalweges - wie HO-1 und GCLC- mit der Western blot - Methode quantifiziert. Weiters wurden die Konzentrationen von BRD4 und dem PDGF-Rezeptor betrachtet, welche in aktivierten glatten Gefäßmuskelzellen erhöhte Konzentrationen aufweisen sollten. Die Ergebnisse zeigten allerdings einen additiven bis synergistischen Effekt der beiden Substanzen bei der Hochregulierung der Nrf2- Zielproteine. Die BRD4 und PDGF-Rezeptor Konzentrationen blieben nahezu unverändert. Weitere Untersuchungen sind daher erforderlich, um die molekulare Ursache des Antagonismus von SFN und JQ1 bezüglich der Proliferationshemmung von glatten Gefäßmuskelzellen näher zu verstehen.

1. Table of Contents

A) Introduction

1) Nrf2

The Nuclear factor erythroid 2-related factor 2 (Nrf2) is a leucine zipper transcription factor which plays a key role in the protection of cells against stressors, for example, reactive oxygen species (ROS), inflammation, radiation, environmental toxins, xenobiotics or the accumulation of misfolded proteins. Under stressed conditions it is stabilized and translocates from the cytosol into the nucleus and binds to its target DNA sequences, which results in the expression of Nrf2 regulated proteins, including those involved in detoxification, redox balance and final stress relief. Thus, the Nrf2 pathway is an interesting target for many inflammatory diseases, such as the chronic obstructive pulmonary disease (COPD), neurodegenerative diseases or diabetes mellitus, i.e. diseases with an etiology connected with (oxidative) stress or disturbed homeostasis (Huang et al., 2015).

Concerning its structure, Nrf2 has seven functional domains, including the DNA binding domain Nrf2-ECH-homology **(Neh)1** or the Kelch-like ECH-associated protein 1 (Keap1) binding domain **Neh2**.
At the Neh1 domain the transcription factor dimerizes with small **Maf** proteins and is then able to bind as a heterodimer to antioxidant response element (**ARE**) sequences in the promoter of target genes. Such target genes include, for example, Heme oxygenase (HO-1) or Glutamate—cysteine ligase catalytic subunit (GCLC).

With ETGE and DLG- two major binding motifs in the Neh2 domain- Nrf2 is able to recruit two molecules of Keap1 under basal conditions. **Keap1** is the important connection between Nrf2 and the ubiquitination ligase Cullin-3 (Cul-3), which recognizes Neh2 and loads its lysines with ubiquitin. Cullin proteins form together with the RING-box proteins (Rbx) the Cullin-RING ubiquitin ligases (E3). The Rbx1

protein recognizes the ubiquitin conjugating enzyme E2, which provides the ubiquitin. E3 ligases the ubiquitins of E2 with the lysines of the target protein, which is Nrf2 in our case. In the end, the target substrate Nrf2 is poly-ubiquitinated and ready for subsequent proteasomal degradation (**Fig. 1**) (Huang et al., 2015; Lydeard et al., 2013).

Upon oxidative insult cysteines on Keap1 get oxidized or covalently modified, which leads to a disconnection between Keap1 and the DLG motif, resulting in the rescue of Nrf2 from ubiquitination and degradation. As a result, Nrf2 accumulates and translocates into the nucleus and acts as a transcription factor. This mechanism is called the 'Keap1-dependent degradation' or the 'canonical pathway'.

Apart from that, other mechanisms, such as posttranslational modifications, acetylation of histones or demethylation of DNA, as well as activating kinases that are able to phosphorylate Nrf2, are only a few examples of ways to boost the Nrf2 abundance.

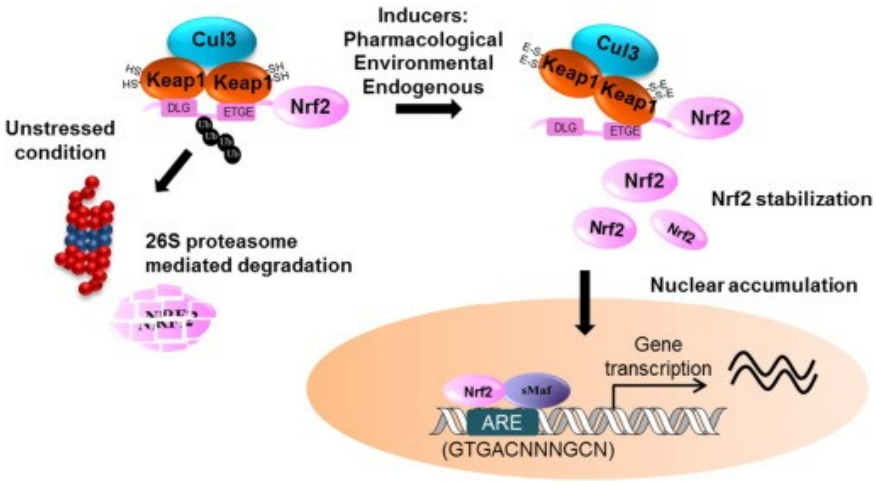

Fig. 1 **Nrf2 signaling pathway**. In unstressed cells Nrf2 is linked to Keap1 via two binding motifs - ETGE and DLG. Two Keap1 molecules are coupled with Cul-3, which initiates proteasomal degradation of Nrf2. Upon activating insults, the connection between Nrf2 and Keap1 is weakened due to the liberation of DLG, which results in accumulation, translocation into the nucleus and gene transcription. Figure adapted from Huang et al., 2015.

Due to its proteasomal degradation and short half-life the transcription factor Nrf2 is usually not very abundant under healthy and resting conditions. Yet, oxidative stress is

not the only way to accumulate and activate the transcription factor. There are lots of phytochemicals (for example Sulforaphane, Curcumin, Quercetin or Xanthohumol), which are also able to influence its stability (Matzinger et al., 2017).

Nrf2 and Atherosclerosis

Atherosclerosis is the narrowing of blood vessels due to the accumulation of e.g. macrophages containing lipids in the inner layer of the artery wall, which is a result of endothelial cells getting damaged by, for example, toxins, high blood pressure or oxidized LDL (oxLDL).
When endothelial cells are damaged vascular smooth muscle cells (VSMC) begin to proliferate (**Fig. 2**) as a response to cytokine release from recruited and activated immune cells and migrate from the tunica media into the tunica intima to form a fibrous capsule over the fatty streak. When the plaque (fatty streak and fibrous capsule) ruptures once, the thrombogenic content is released and leads to thrombosis, which interrupts blood flow and causes, for example, myocardial infarction (Di Pietro et al., 2016; Marx et al., 2011).

Nrf2 plays an important role in the prevention of atherosclerosis. It protects macrophages from oxLDL mediated injury by upregulation of antioxidant enzymes. For example, the antioxidant enzymes HO-1 and GCLC both play an important role in the defense of atherosclerosis. HO-1 overexpression inhibits atherosclerotic lesion formation and its downregulation aggravates it (Juan et al.,2001; Yet et al.,2003). The same is with GCLC, which leads to higher glutathione levels, thereby protects the endothelial cells from oxLDL-induced oxidative damage and also decreases atherosclerotic lesion formation (Zhu et al., 2008).

There is also evidence that Nrf2 target genes such as Ho-1, NQO1 and sequestosome-1 (SQSTM1) supress SMC proliferation (Cho et al., 1999). The reduction of reactive oxygen species through Nrf2 activation is also considered as a supporting mechanism to VSMC proliferation inhibition (Bai et al., 2015).

Another anti-atherogenic effect of Nrf2 is the suppression of various tumor necrosis factor alpha (TNFα) induced actions in the early stage of atherosclerosis. TNF-alpha is

responsible for the expression of the adhesion molecules VCAM-1 and ICAM-1, which mediates the adhesion of monocytes to vascular endothelium and is therefore involved in endothelial cell (EC) activation (Mimura et al., 2015; Bai et al., 2015).

However, there is also evidence for a proatherogenic effect of Nrf2, as studies reported that Nrf2 induces CD36 scavenger receptor expression in macrophages, which is responsible for the uptake of oxLDL and the foam cell formation of macrophages. Regarding lipid concentrations, Nrf2 activation also shows contradictory results depending on study design and readout, indicating that there is still much to investigate to understand the complex mechanism of Nrf2 activation and atherosclerosis (Mimura et al., 2015).

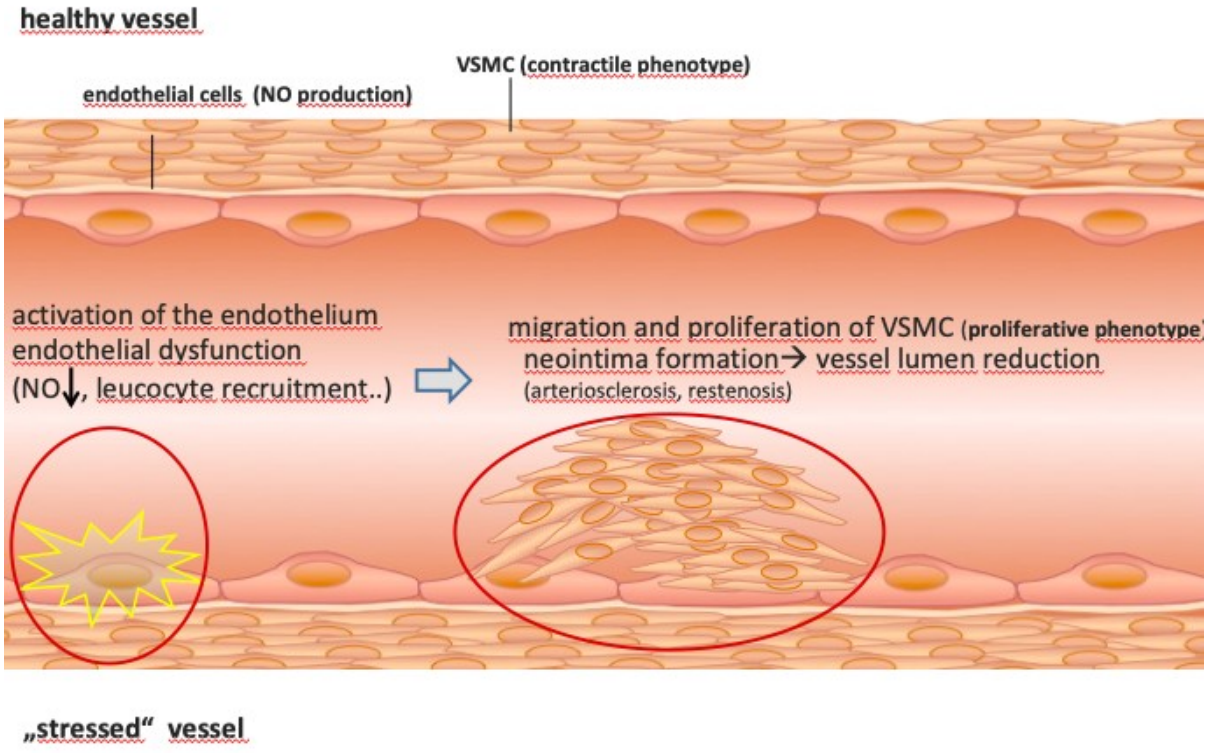

Fig. 2 **Healthy and stressed blood vessels.** In healthy vessels VSMC are contractile and endothelial cells are able to produce the vasodilating nitrogen monoxide (NO). In stressed vessels the activation of the endothelium leads to endothelial dysfunction and results in a diminished NO release and in leucocyte recruitment. As a consequence, VSMC begin to proliferate and migrate into the tunica intima (proliferative phenotype), which contributes to atherosclerosis and restenosis by narrowing the vessel lumen.

2) Sulforaphane

Sulforaphane (SFN) is a well-studied chemopreventive isothiocyanate which is found in cruciferous vegetables of the Brassica genus, such as broccoli, cauliflower or brussel sprouts. In foods it exists as a glycoside known as glucoraphanine, which is converted to its biologically active form, Sulforaphane, by an enzyme called myrosinase (**Fig. 3**). The hydrolysis of glucoraphanin is achieved either by plant myrosinase in the vegetable itself or bacterial myrosinase in the human colon (Kensler et al., 2013).

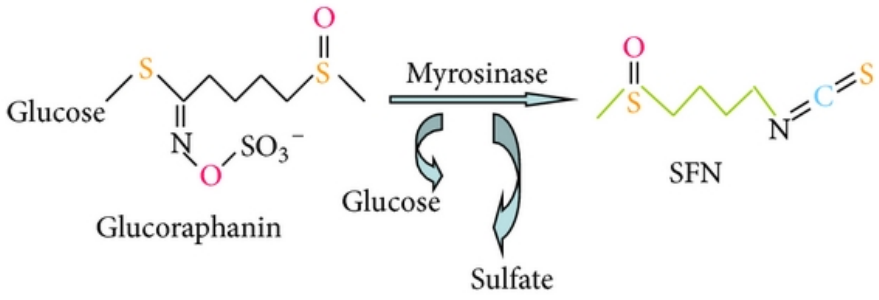

Fig. 3 **Hydrolysis of glucoraphanin.** Glucoraphanine is hydrolyzed by the enzyme myrosinase to glucose, sulfate and Sulforaphane. Figure adapted from Bai et al., 2015.

Activation of the Nrf2 pathway by Sulforaphane

a) Keap1 dependent activation

Modifying cysteine groups of Keap1 prevents proteasomal degradation of Nrf2 by a diminished interaction between Keap1 and Cul-3.
Sulforaphane is one of numerous plant-derived compounds, which is able to reversibly

react with its electrophilic isothiocyanate group with sulfhydryl groups of Keap1 cysteines (**Fig. 4**).

Hu et al. (2011) tested the reactivity of all 27 Keap1 cysteine groups towards SFN and reported that the most readily modified Keap1 cysteines were C38, C151, C368 and C489. Furthermore, taking into account that lots of other investigators proved that Keap1-dependent Nrf2 activation by SFN greatly depends on the Cys151 residue, these results show that modification of cysteine residues with Sulforaphane is responsible for releasing Nrf2 from Keap1-pursued proteasomal degradation (Eggler et al., 2009; Takaya et al., 2012; Zhang and Hannink, 2003).

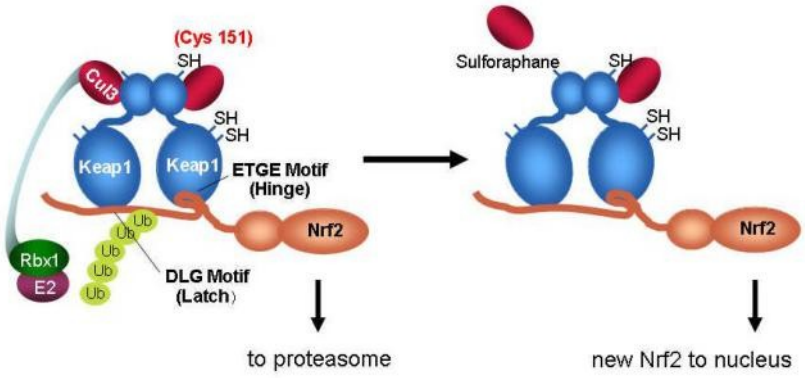

Fig. 4 **Keap1 dependent Nrf2 activation of SFN.** Under unstressed conditions Nrf2 is marked for proteasomal degradation through the Cul-3/Rbx1/E2 ubiquitin ligase complex. Upon treatment with SFN the interaction of Keap1 with Cul-3 (due to the occupation of Keap1 sulfhydryl groups by SFN) is interrupted. Nrf2 can accumulate and translocate into the nucleus. Figure adapted from Kensler et al., 2013.

b) Translational regulation

Li et al. (2009) reported that the human Nrf2 messenger ribonucleic acid (mRNA) contains an internal ribosomal entry site (IRES) at the 5' untranslated region. IRES contains an 18S rRNA binding site (RBS), which - as a part of the small eukaryotic ribosomal subunit (40S) - is required for the initiation of polysomal translation. The investigators could also show that the treatment with Sulforaphane enhances $IRES_{Nrf2}$ driven translation. Accordingly, Sulforaphane enhances protein synthesis of Nrf2 and contributes to its activity also in a Keap1 independent manner.

c) Epigenetic regulation

Epigenetics is the study of gene expression / phenotype changes without altering the DNA sequence itself. It includes DNA methylations and histone modifications, which have an essential influence on gene activity. In general, hyperacetylated histones result in high transcriptional activation by loosening the chromatin, whereas methylated DNA is transcriptionally less active.

Zhang et al. (2013) demonstrated that Sulforaphane leads to demethylation of CpGs (cytosine - phopshate - guanine) in the Nrf2 promoter regions as well as to a decrease of DNA methyl-transferases DNMT1 and DNMT3a. They further showed that SFN reduces the protein expression levels of several histone-deacetylases (HDAC) and increases acetyl - histone 3 levels (Ac-H3). Thus, Sulforaphane furthermore boosts Nrf2 abundance by epigenetic regulation.

d) Inactivation of GSK3β/TrcP

Shang et al. (2015) proved that, in diabetic rats, the inhibitory Serine 9 (Ser9) phosphorylation of the glycogen synthase kinase 3 beta (GSK3β) is reduced, leading to its activation. Sulforaphane was able to counteract this effect and keep GSK3β in a more inactive state. Notably, GSK3β is a kinase reported to be able to phosphorylate a group of Serine residues in the Neh6 domain of Nrf2 and lead to its beta-transducin

repeat containing E3 ubiquitin protein ligase (β-TrCP)-mediated proteasomal degradation (Rada et al., 2012). Thus, the inactivation of GSK3β by Sulforaphane treatment augments Nrf2 levels by preventing its β-TrC- mediated degradation.

e) Phosphorylation of ERK

Mitogen activated protein kinases belong to the superfamily of serine/threonine kinases and play a central role in transducing extracellular signals into the nucleus. They therefore have an influence on gene expression, cell proliferation, differentiation and cell death.

Yu et al. (2000) reported that the MAPK pathway is involved in Nrf2 - mediated antioxidant gene expression. Inactivating this pathway with specific inhibitors showed reduced expression of ARE-dependent detoxifying enzymes.
In this study, Sulforaphane induced phosphorylation of the extracellular signal-regulated kinase (ERK1/2) and had an influence on the activation of Raf-1 kinase as well as MAPK kinase (=MEK1/2 or MAP2K), indicating that Sulforaphane contributes to Nrf2 signaling by activating these kinases, which then leads to Nrf2 phosphorylation, accumulation and entry into the cell nucleus.

Overall, Sulforaphane can boost Nrf2 activity by elevating Nrf2 gene expression, increasing Nrf2 protein abundance and favouring activating phosphorylations on Nrf2.

Prevention of Atherosclerosis with Sulforaphane

SFN may play an important role in the protection against atherosclerosis in many ways. It is reported to inhibit the platelet derived growth factor (PDGF)-induced **VSMC proliferation** by arresting them at the G1/S phase of the cell cycle through the up-upregulation of the tumor suppressor p53 and the cell cycle inhibitor p21 (Shawky and Segar, 2017). Sulforaphane also leads to **enhanced HO-1** expression and **reduces ROS levels** via Nrf2, suggesting that the Nrf2 activation by SFN may play a key role for

VSMC proliferation inhibition since HO-1 expression leads to a cell cycle arrest at the G1 phase due to its end products carbon monoxide and bilirubin and since ROS is associated with enhanced VSMC proliferation (Wang et al., 2018; Ollinger et al., 2005; Otterbein et al., 2003).

Activation of the mechanistic target of rapamycin (mTOR)/p70S6K pathway also contributes to VSMC proliferation. A recent study showed that Sulforaphane treatment leads to a decreased PDGF-induced phosphorylation of p70S6K/S6 and cyclin D1 (which is important for the G1/S phase transition) **independent of Nrf2**. It is very important that this study also showed that Nrf2 downregulation did not alter SFN induced inhibition of p70S6K/S6 or cyclin D1 (Shawky and Segar, 2017). In addition, Ashino et al. (2013) showed that the down-regulation of Nrf2 enhances PDGF - stimulated VSMC migration but not VSMC proliferation, again indicating that the activation of Nrf2 may not be essential for SFN-induced VSMC proliferation inhibition. Thus, it would be necessary to further investigate whether Nrf2 really plays an essential role for the inhibition of VSMC proliferation by Sulforaphane.

Taken together, SFN inhibits VSMC proliferation a) by the up-regulation of p53 and p21, which results in a G1 arrest; b) by inhibiting the PDGF induced p70S6K/S6 phosphorylation; and c) presumably less pronounced by several Nrf2-induced mechanisms, such as induced HO-1 expression or ROS reduction.

However, SFN still owns many anti-atherogenic actions by activating the Nrf2 pathway in other cell types, leading to **VCAM-1 repression**, **HO-1** and **GCLC expression** or **ROS reduction** (Bai et al., 2015) in endothelial or immune cells. How these mechanisms could prevent atherosclerosis are described in chapter "Nrf2 and atherosclerosis".

SFN may further prevent atherosclerosis by **inhibiting platelet aggregation**, especially by collagen inhibition, which activates GPIIb/IIIa and thromboxane A and contributes to platelet aggregation. Furthermore, SNF also reduces the TNF-α induced endothelial lipase expression, which **decreases HDL** cholesterol levels and thereby promotes atherosclerosis (Bai et al., 2015).

In line with these reported molecular mechanisms, SFN is reported to successfully reduce neointima formation and restenosis after balloon injury in vivo (Kwon et al., 2012).

3) BRD4

There are three types of epigenetic regulators, all of which are able to control transcriptional activity: a) the writers, which lead to histone or DNA modifications, b) the erasers, which are able to remove these modifications, and finally, c) the readers, which are able to recognize and/or bind to the modifications. Bromodomain proteins belong to the third group of epigenetic regulators; hence, they play an important role in regulating gene expression by recognizing acetyl residues.
Bromodomains are present, for example, in histone acetyl-transferases and methyl-transferases, transcriptional co-activators, chromatin-associated proteins and the bromodomain and extraterminal domain family (**BET**), which has become the most important and intensely studied bromodomain group in the last few years. The BET subfamily is localized in the nucleus and comprises the bromodomain-containing proteins (BRD) BRD2, BRD3 BRD4, which are expressed ubiquitously, and BRDT in male germ cells. BRD4 is a promising therapeutic target as it is recruited by **super-enhancers** upon pathogenic stimulation and activates the transcription of several genes associated with diseases. Therefore, **BRD4** is reported to be **up-regulated** in several cancers and various inflammatory diseases, such as leukemia, breast cancer, cardiovascular diseases or diabetes.

BRD4 has two bromodomains (BD), BD1 and BD2, whereby it is able to bind to specific acetylated lysine residues **on histones and non-histone proteins**. In short, BRD4

a) is an epigenetic regulator not only due to its ability to 'read' the acetylation code but also due to its histone acetyl-transferase (**HAT**) activity;

b) directly influences transcriptional activity by phosphorylating and activating the positive transcription elongation factor (P-TEFb), as well as RNA polymerase II and the transcription initiation factor TFIID subunit 7 (TAF7), thereby activating the transcriptional machinery;

c) indirectly influences transcriptional activity by being a scaffold for several transcription factors and assisting the elongation of distal **enhancer RNAs;**

d) plays a role in cell cycle progression by recruiting P-TEFb to promoters of early G1 genes during telophase;

e) plays an important role in normal cell differentiation and development, as well as the regulation of genes (for instance, Myc) that are involved in cancer development (Tomomi Noguchi-Yachide, 2016).

4) JQ1

(+)- JQ1, a triazolothienodiazepin, is a reversible and selective BET inhibitor (**Fig. 5**). Once bound to an asparagine in BRD4, a hydrogen bond is formed between the triazolo - group of JQ1 and a tyrosine in BRD4, impairing the interaction between BRD4 and its target acetyl lysine residues. JQ1 is investigated extensively as it leads to BRD4 inhibition, and thereby to down-regulation of several cancer-associated genes (Tomomi Noguchi-Yachide, 2016).

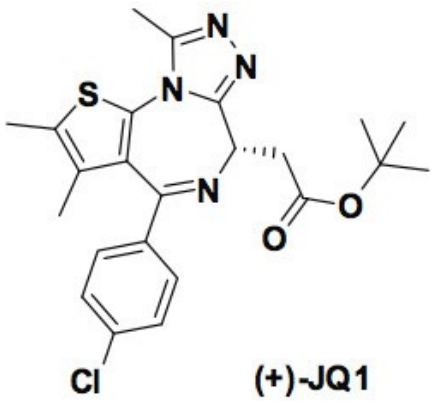

Fig. 5 **The active enantiomer of JQ1.**
Figure adapted from Matzuk et al., 2012.

For instance, JQ1 shows anti-proliferative effects in Burkitt's lymphoma, acute myeloid leukemia (AML), acute lymphoblastic leukemia (ALL) and multiple myeloma (MM) cells especially through the down-regulation of the oncogene **c-Myc** (Di Costanzo et al., 2014).

Besides, JQ1 **inhibits** the BRD4-driven activation of the nuclear factor kappa B (**NF-κB**) dependent inflammatory genes. As a result, it decreases the secretion of cytokines, such as TNF-α, Interleukin 1 beta (IL-1β), IL-6 and IL-8, and therefore is a promising

target in inflammatory diseases. Also, JQ1 inhibits angiogenesis by reducing the NF-κB activated angiogenic factor VEGF (Ferri et al., 2016).

Leading to differentiation, G1 arrest and apoptosis in nuclear protein in testis (NUT) midline carcinoma cells as well as reducing invasion and migration of breast cancer cell lines are only a couple of additional examples of JQ1's possible wide range of bioactivities (White et al., 2019).

JQ1/BRD4 and atherosclerosis

VSMC proliferation occurs after a phenotype switch of VSMC from a quiescent to a proliferative and migratory cell state, which is reported to be regulated by chromatin remodeling (Alexander and Owens, 2012).
Angiotensin II (AngII) up-regulates several genes that are involved in VSMC proliferation. Das et al. (2017) reported that AngII-mediated hypertension and VSMC proliferation and inflammation are regulated by super-enhancers and that JQ1 ameliorates these AngII-mediated actions by blocking the super-enhancer formation. Upon AngII treatment the promoters of these genes show enhanced enrichment of acetylated histones as well as BRD4, which leads to transcriptional activation. However, **JQ1 attenuates AngII-regulated super enhancer formation** by occupying the BRD4 binding sites. It therefore prevents AngII-mediated actions, as well as the phenotypic switch of VSMC to a proliferative cell state.

Apart from that, Wang et al. (2015) showed that **BRD4** is dramatically **up-regulated** during neointima formation in injured rat and human blood vessels and that PDGF stimulation increased BRD4 protein levels in rat aortic smooth muscle cells. They showed that JQ1 treatment or BRD4 knockdown **reduced intimal hyperplasia** and **inhibited** PDGF stimulated **SMC proliferation and migration**. In addition, JQ1 also prevented cytokine-induced apoptosis of endothelial cells unlike standard drugs like rapamycin in drug-eluting stents.

Taken together, JQ1 prevents the BRD4-driven phenotypic transition of VSMC to a proliferative and migratory cell state, hence it is responsible for inhibiting VSMC

proliferation and migration, as well as AngII-mediated hypertension. Therefore, JQ1 is a potential lead compound for the treatment and prevention of atherosclerosis/restenosis and has to be studied in more detail in future studies.

5) Regulation of the Nrf2 pathway by BRD4

Several studies have shown that BRD4 knockdown or JQ1 treatment leads to the activation of Nrf2-dependent target genes, indicating that **BET-proteins negatively regulate the Nrf2 pathway.**
By way of example, it was reported that JQ1 increases protein and mRNA levels of Nrf2, as well as the Nrf2-dependent antioxidant enzymes NAD(P)H dehydrogenase (quinone) 1 (NQO1), GCLC and HO-1 in aortic smooth muscle cells and several cancer cell lines (Michaeloudes et al., 2014). Therefore, the combinatorial treatment of Nrf2 activators and BET inhibitors in inflammatory diseases should be investigated in future studies (**Fig. 6**), especially due to enhanced activation of the Nrf2 tarfet gene NQO1 upon combinatorial treatment with Sulforaphane and JQ1 observed in clinical trials (Chatterjee et al., 2016).

To understand the underlying mechanism of JQ1-driven Nrf2 activation, Chatterjee et al. (2016) investigated whether the inhibitory effect of BRD4 on Nrf2 is Keap1-dependent or whether it depends on the direct protein-protein interaction between Nrf2 and BRD4. They proved that the Cap'n'collar isoform C (CncC), the fly ortholog of Nrf2, is a **substrate for acetylation/deacetylation** and that the female sterile homeotic (Fs(1)h), the BET-protein in Drosophila, binds to acetylated lysine residues on CncC, thereby inhibiting its effects. In general, acetylated Nrf2 is reported to be more active (Kawai et al., 2010) but it apparently loses its activity by interacting with BET-proteins.

The investigators also showed that JQ1 interrupts the interaction between BET-proteins and acetylated Nrf2 and leads to subsequent Nrf2 activation. It is also important that BRD4 regulates Nrf2 at the post-translational level, which means that BRD4 only interacts with the Nrf2 protein and not its mRNA. The direct interaction between BRD4 and the Nrf2 protein was also observed in human cell lines by other

investigators, which means that **BRD4 negatively influences the Nrf2 pathway by occupying the acetylated lysine residues on the Nrf2 protein**. It therefore leads to down-regulation of several Nrf2 regulated antioxidant proteins (Guo et al., 2015; Michaeloudes et al., 2014).

However, the enhanced Nr2 activation is not always of advantage, since Nrf2 plays a dual role when it comes to cancer. While Nrf2 activation prevents chemical carcinogenesis in various premalignant tissues, cancer cells can also misuse Nrf2 activation in order to protect themselves against oxidative stress caused by cytostatic drugs or radiation therapy. AML cells are an example of cancer cells protecting themselves against oxidative stress through Nrf2 signaling. Therefore, since BET-proteins contribute to AML, inhibiting the Nrf2 pathway combined with BET-protein inhibitors may show enhanced cytotoxicity (**Fig. 6**).

However, a recent study showed that the combinatorial treatment with Sulforaphane and JQ1 leads to enhanced inhibition of colon cancer cell proliferation (Rajendran et al., 2019), indicating that not all cancer cells may use Nrf2 signaling to protect themselves against stressors or that also Nrf2 independent mechanisms play a major role. In this study Sulforaphane induced new acetylation sites on a non-histone protein called CCAR2 (cell cycle and apoptosis regulator 2). The new acetylation sites on CCAR2 interacted with BET member proteins BRD2, BRD3 and BRD9. However, this interaction was interrupted by JQ1, leading to a synergistic effect in colon cancer cell proliferation inhibition.

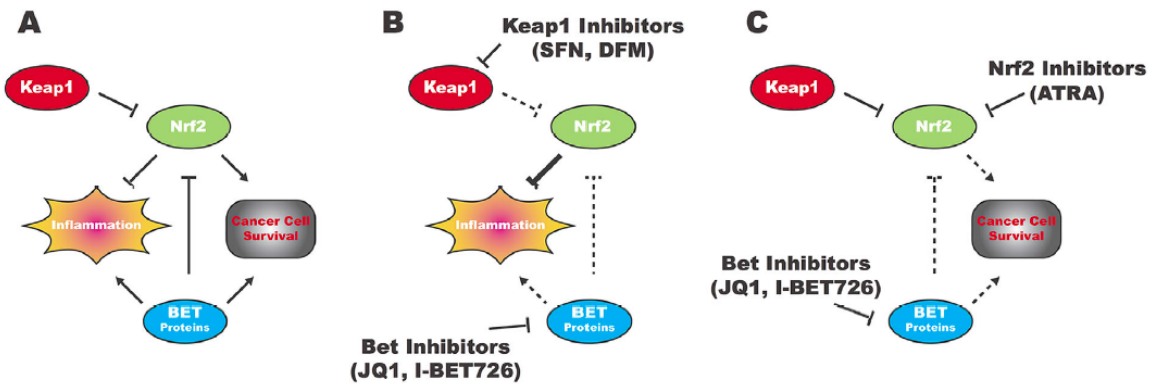

Fig. 6 **How to combine Nrf2 activators and BET inhibitors in cancer cells and inflammatory diseases**. A) Nrf2 activation and BET-proteins inhibit inflammation but can also provide cancer cell survival. B) For inflammatory diseases BET inhibition should be combined with Keap1 inhibitors such as SFN, in order to enhance Nrf2-dependent anti-inflammatory signaling. C) In cancer cells BET inhibitors together with Nrf2 inhibitors may show a synergistic effect by preventing cancer cells from Nrf2-dependent protection against oxidative stress. Picture adapted from Chatterjee and Bohmann, 2018.

6) Aim of the Work

The aim of this diploma thesis is to find out whether the BET inhibitor JQ1 can enhance the inhibition of VSMC proliferation brought about by the Nrf2 – activator Sulforaphane (**Fig. 7**).

For this, IC_{50} for the individual compounds in VSMC proliferation were determined with the crystal violet assay, followed by combinatorial treatment with JQ1 and SFN in VSMC to see if the inhibition of VSMC proliferation could then be enhanced. Additionally, the cell cycle distribution upon treatment of SFN and JQ1 was examined by flow cytometry.
Moreover, expression of target proteins of the NRF2 pathway, such as HO-1 and GCLC, as well as BRD4 and PDGF- R levels were determined by using the western blotting technique.

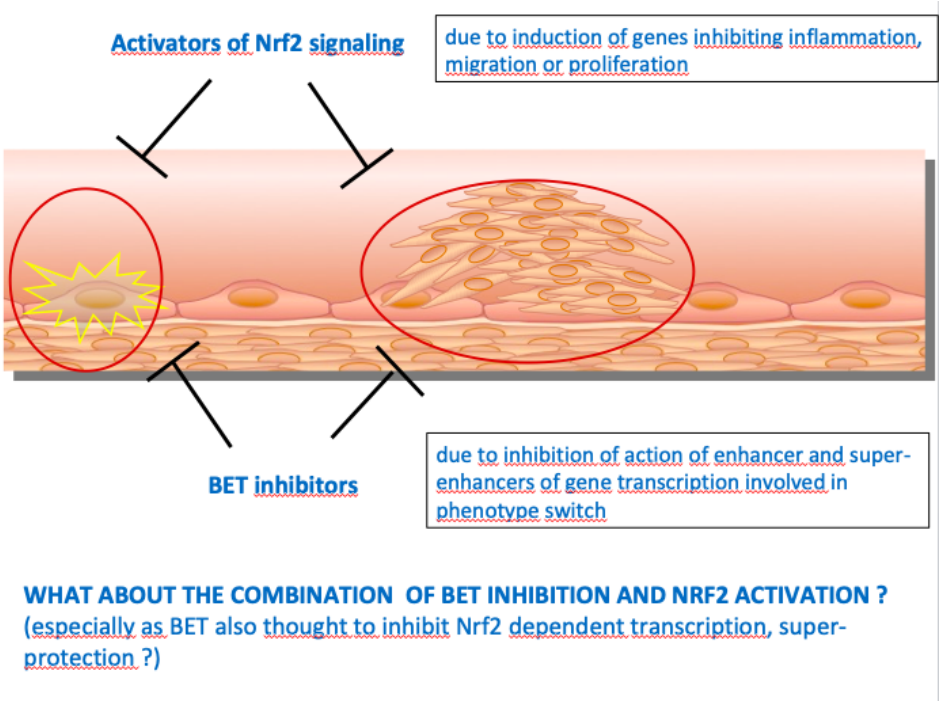

Fig. 7 **Possible enhanced VSMC proliferation inhibition by combinatorial treatment of BET inhibitors and Nrf2 activators.** Nrf2 activators partly inhibit VSMC proliferation by the up-regulation of Nrf2 target genes, whereas BET inhibitors, such as JQ1, inhibit proliferation by preventing super enhancer formation, which is associated with the phenotype transition of VSMC to a proliferative cell state. Therefore, a combination of Nrf2 activators and BET inhibitors could lead to an enhanced VSMC proliferation inhibition.

B) Materials & Methods

1) Materials

a) Cell culture reagents and solutions

NAME	PROVIDER
DULBECCO'S MODIFIED EAGLE'S MEDIUM (DMEM)	Lonza Group Ltd.
HAMS F12	Lonza Group Ltd.
GENTAMYCIN/AMPHOTERICIN B	Lonza Group Ltd.
FETAL BOVINE SERUM (FBS)	Gibco® by life technologies™
DIMETHYL SULFOXIDE (DMSO)	Sigma® Life Science
PDGF-BB	Bachem (Germany)
PHENOL RED	Sigma® Life Science

NAME	INGREDIENTS		STORED AT
GROWTH MEDIUM	DMEM/Hams F12 (1:1)	500 ml	4° C
	Fetal Bovine Serum	20 %	
	Gentamycin / Amphotericin B	1 %	
	Phenol red	1.5 ml	
STARVATION / DIET MEDIUM	DMEM/Hams F12 (1:1)	500 ml	4° C
	Fetal Bovine Serum	0.1 %	
	Gentamycin / Amphotericin B	1 %	
	Phenol red	1.5 ml	
PHOSPHATE BUFFERED SALINE (PBS)	NaCl	36 g	4° C
	Na_2HPO_4	7.4 g	
	KH_2PO_4	2.15 g	
	Aqua destillata	5000 ml	
TRYPSIN/EDTA	Trypsin	0.5 g	-20° C
	Na_2EDTA	0.2 g	
	PBS	1000 ml	

b) Solutions and reagents for crystal violet assay

NAME	INGREDIENTS	STORED AT
PDGF-BB	200ng/20µl stock solution dissolved in sterile aqua bidest. (10%), PBS and 0.2% BSA (90%)	4° C
CRYSTAL VIOLET SOLUTION	Crystal violet 1 % Methanol 20 % Aqua Dest. 80 %	4° C
ETOH/CITRATE SOLUTION	EtOH 50 % Sodium citrate solution 50 %	RT (room temperature)

c) FACS buffer and reagents

NAME	INGREDIENTS
FACS BUFFER (5 L, PH = 7.37)	NaCl 40.6 g KH_2PO_4 1.3 g Na_2HPO_4 11.75 g KCl 1.4 g LiCl 2.15 g NaN_3 1 g Na_2EDTA 1.8 g
PROPIDIUM IODID SOLUTION	Triton X-100 0.1 % (v/v) Sodium citrate 0.1 % (v/v) Propidium iodid 50 µg/ml

d) Western blotting materials

NAME	INGREDIENTS
LYSIS BUFFER	RIPA-Buffer 2500 µL Complete® 100 µL PMSF 50 mM 25µL Natriumorthovanadat 100 mM 50 µL Natriumfluoride 1 M 125 µL Natriumpyrophosphate 100 mM 125 µL
RIPA BUFFER	NaCL 438.3 mg TRIS-HCL 394 mg Nonidet P 40 500 mg Deoxycholic acid sodium salt 125 mg SDS 50 mg Ad. 50 mL Aqua dest.
BRADFORD REAGENT	Roti®-Quant (Carl Roth GmbH)
SDS SAMPLE BUFFER (3X)	0.5M TRIS-HCL pH 6.8 37.5 mL SDS 6 g Glycerol 30 ml Bromophenol blue 15 mg Ad 100 mL Aqua dest. Before use: Stock solution + 2-Mercaptoethanol (15%)
SEPARATION GEL (10%, AMOUNT FOR 2 GELS)	PAA 30 % 5.0 ml 1.5 M Tris-HCL, pH 8.8 3.75 ml 10 % SDS 150 µl dd H_2O 6.1 ml directly before use: TEMED 15 µl APS (10 %) 75 µl
STACKING GEL (AMOUNT FOR 2 GELS)	PAA 30 % 1.28 ml 1.25 M Tris-HCL, pH 6.8 750 µl 10 % SDS 7.5 µl

	dd H_2O 5.25 ml directly before use: TEMED 15 µl APS (10 %) 75 µl
ELECTROPHORESIS BUFFER (10X)	TRIS-Base 30 g Glycine 144 g SDS 10 g Ad 1000 mL Aqua dest.
BLOTTING BUFFER	Blotting Buffer (5X) 100 ml MeOH 100 ml Aqua dest. 300 ml
BLOTTING BUFFER (5X)	TRIS-Base 15.169 g Glycine 72.9 g Ad 1000 mL Aqua dest.
TBS-T	Tris-Base 3.0 g NaCL 11.1 g Tween 20 1 ml Ad 1000 mL Aqua dest.
5 % BSA - SOLUTION	Bovine Serum Albumin 2.5 g PBS ad 50 ml
ECL	H_2O 4.5 ml 1 M TRIS-Base (pH 8.5) 0.5 ml Luminol 25 µL P - Coumaric acid 11 µL H_2O_2 3 µL
LUMINOL	Luminol 0.44 g DMSO 10 mL
P - COUMARIC ACID	P - Coumaric acid 0.15 g DMSO 10 mL
COMPLETE®	Complete® 1 tablet Aqua dest. 2000 µL

Primary Antibodies

TARGET	MANUFACTURER	ORIGIN	STORAGE	MONO-/ POLYCLONAL	DILUTION
HO-1	Enzolifesciences	rabbit	4° C	polyclonal	1:1000
PDGF-R BETA	Cell signaling technology	rabbit	- 20 °C	monoclonal	1:1000
BRD4	Abcam	rabbit	4° C	monoclonal	1:1000
GAMMA-GCSC	Santa Cruz	mouse	4° C	monoclonal	1:300
AKTIN	mpbio	mouse	- 20 °C	monoclonal	1:5000

Secondary Antibodies

TARGET	MANUFACTURER	STORAGE	DILUTION
ANTI RABBIT IGG, HRP-LINKED ANTIBODY	Cell signaling technology	-20 ° C	1:1000
ANTI MOUSE IGG, HRP-LINKED ANTIBODY	Cell signaling technology	- 20 ° C	1:1000

e) Software

NAME	PROVIDER
GRAPHPAD PRISM 4	GraphPad Software Inc.
VI-CELL™ XR 2.03	Beckman Coulter Inc.
BD CELLQUEST™ PRO	Becton, Dickinson and Company
MULTI GAUGE V3.0	Fujifilm, Tokyo, Japan
IMAGE READER LAS-3000™	Fujifilm, Tokyo, Japan
MICROSOFT® OFFICE EXCEL 2013	Microsoft

f) Technical Equipment

NAME	PROVIDER
HERASAFE™ KS WORKBENCH	Thermo Fisher Scientific Inc.
HERACELL™ 150 INCUBATOR	Thermo Fisher Scientific Inc.
JULABO SW23 SHAKING WATHER BATH	JULABO GmbH
VI-CELL™ XR CELL VIABILITY ANALYZER	Beckman Coulter Inc.
GALAXY MINI MICROCENTRIFUGE	VWR International Inc.
HERAEUS™ MULTIFUGE™ 1 S-R CENTRIFUGE	Thermo Fisher Scientific Inc
TECAN SUNRISE™ (96-WELL-PLATE READER)	TECAN, Mannedorf, Switzerland
FACSCALIBUR™	BD Biosciences Pharmingen
VORTEX SHAKER	VWR International Inc.
LAS-3000™ (LUMINESCENT IMAGE ANALYZER)	Fujifilm, Tokyo, Japan
RCT BASIC MAGNETIC STIRRER	IKA™ Laboratory equipment
OLYMPUS CKX41 LIGHT MICROSCOPE	Olympus Europe GmbH
VIBRAX VXR BASIC SHAKER	IKA™ Laboratory equipment
HERAEUS™ FRESCO™ CENTRIFUGE	Thermo Fisher Scientific Inc.

g) Miscellaneous

NAME	PROVIDER
TISSUE CULTURE FLASK 175 CM^2	Sarstedt GmbH
TISSUE CULTURE FLASK 75 CM^2	Sarstedt GmbH
96-WELL MICROTITERPLATES	Greiner bio-one
6-WELL MICROTITERPLATES	Greiner bio-one
SEROLOGICAL PIPETTES (1ML, 2ML, 5ML, 10ML, 25ML)	Sarstedt Gmb
SEROLOGICAL PIPETTE TIPS (10µL, 200µL)	Sarstedt GmbH
SEROLOGICAL PIPETTE TIPS (1000µL)	Greiner bio-one
EPPENDORF® RESEARCH PLUS PIPETTES	Eppendorf GmbH
EPPENDORF® RESEARCH PLUS PIPETTES (MULTICHANNEL)	Eppendorf GmbH
EPPENDORF® RESEARCH PLUS PIPETTE TIPS (MULTICHANNEL)	Eppendorf GmbH
TISSUE CULTURE DISHES (6 CM)	Greiner bio-one
NITROCELLULOSE MEMBRANE	Bio-Rad Laboratories, Inc
CELL SCRAPER	Greiner bio-one

2) Methods

a) Cell culture

Cells

For all experiments cryopreserved primary vascular smooth muscle cells isolated from the aorta of adult Sprague Dawley rats from Lonza Group Ltd. were used.

Cell culture

All of the cell culture steps were taken under aseptic conditions by using sterile pipettes, media and reagents, and by working under a Laminar Air Flow workbench. Since cold media can cause damage to cells all the solutions were pre-warmed at 37° C for 10-15 minutes before beginning work. The cells were cultured at 37° C and 5% CO_2 in 75 cm^2 flasks or 175 cm^2 flasks.

Passaging cells

Passaging cells is an important step in cell culture, which is performed by transferring an aliquot of cells from one flask to a new flask with fresh medium.
Therefore, the growth medium (GM) has to be removed from the culture vessel. After washing with PBS (10 mL for 75 cm^2 flask / 20 mL for 175 cm^2 flask), a serine protease called Trypsin (3 mL for 75 cm^2 flask / 5-6 mL for 175 cm^2 flask) was added to free the adherent cells from the ground. To speed up the cell detachment, cells were incubated for 3-5 minutes at 37°C and 5% CO_2. Growth medium (7 mL for 75 cm^2 flask / 12 mL for 175 cm^2 flask), which contains FBS, was added to stop the activity of Trypsin (otherwise the digesting effect of Trypsin would damage the cells). 1 mL of cell suspension was added into a tube in order to count the number of cells with the hemocytometer ViCell XR®. The volume for the desired cell number is added into a new flask with fresh growth medium (13 mL for 75 cm^2 / 30 mL for 175 cm^2).

Cells were passaged twice a week. 1 – 1.5 million cells were passaged from Monday to Friday in a 75 cm^2 culture flask and 2.5 - 3 million from Friday to Monday in a 175 cm^2 flask.

Only the cells between the 6^{th} and 18^{th} passage were used for the experiments. After the 18^{th} passage the cells were disposed and a new cryovial of frozen cells, which were stored in liquid nitrogen, was taken out. The nearly thawed cell suspension has to be diluted quickly with growth medium to dilute the DMSO concentration (5-10%) contained in the freezing medium . Therefore, after defrosting the cell suspension (approx. 1 million cells in 1 ml freezing medium) in the water bath at 37° C, the cells were immediately added into a falcon filled with pre-warmed growth medium and transferred into a flask to incubate until the next passage.

Heat inactivation of FBS

The heat inactivation of serum is performed to inactivate the complement system, which may otherwise cause damage to the cells or unwanted changes in cellular signalling if they were to be treated with serum that was not heat inactivated.
To perform the heat inactivation, FBS was thawed at 37° C in the water bath. Meanwhile another water bath was heated to 58° C. FBS and a reference water bottle with a thermometer was then placed into the water bath that was heated to 58°C. When the thermometer had reached 56°C, the temperature of the water bath was adjusted to 56° C and the serum was kept for 30 minutes in the water bath. FBS was then aliquoted into 50 mL falcons and stored at – 20° C.

b) Crystal violet assay

Introduction

The crystal violet assay is commonly used to determine the amount of cells in multi well-cluster dishes. Crystal violet is a simple biomass stain. The number of adherent cells in a well is directly proportional to the bound dye. Thus, this method allows comparative appreciation of cell division (→ more cells→ more bound dye) or death (→ cell detachment → less bound dye) between different wells by quantification of dye absorbance in a spectrophotometer (Feoktistova et al., 2016).

To perform the crystal violet assay cells were seeded in 96-well plates. 100 µL of the prepared cell suspension, containing 500 000 cells in 10 mL GM, was added into the wells with a multi-channel pipette. Eventually, each well contained 5000 cells dissolved in 100 µL GM.

On the next day, the cells were washed two times with PBS. 100 µL of starvation medium (ST) was added to synchronize the cell cycle. The cells were starved for approximately 24 hours.

Treatment of cells

<u>Single treatment</u>
3 Falcons with 3 mL of ST / GM / ST + PDGF (40 ng/mL) were prepared. The stock solution of PDGF had a concentration of 200 ng/20 µL, of which 12 µL were added into 3 mL of ST to have a concentration of 40 ng/mL.
Then, eppendorf tubes with 5x 500 µL of ST/ GM / ST + PDGF (40ng/ml) for each compound was prepared. 1 µL of the prepared stock solutions were added into the eppendorf tubes. The concentrations of the prepared stock solutions were:
SFN: 25 mM, 10 mM, 5 mM, 2,5 mM, 0 mM
JQ1: 1 mM, 0.5 mM, 0.25 mM, 0.125 mM, 0 mM

100 µL of each solution was added into 4 wells of the 96 well plate. The 96-well plates were incubated for about 48 hours at 37°C and 5 % CO_2.

Combinatorial treatment in serum

1 falcon with 1.5 mL ST and 1 falcon with 1 mL GM was prepared, of which 100 µL was added into the wells that should not be treated with any compound (see pipetting pattern: starvation, +10% serum). The single treatment of SFN and JQ1 was done as described above (only with other concentrations).

5 falcons with 5 mL GM and 20 µM, 10 µM, 5 µM, 2.5 µM and 0 µM of SFN were prepared. Of this solution, 500 µL were added into eppendorf tubes for each different concentration of JQ1 (=5 x 500 µL).
To prepare the stock solution of JQ1, 5 eppendorf tubes were prepared with the concentrations of 100 µM, 200 µM, 400 µM, 600 µM, 800 µM. 1 µL of the JQ1 stock solutions were added into each eppendorf tube in which SFN was already dissolved.

100 µL of each solution of the eppendorf tube was added into 4 wells of the 96 well plate. The 96-well plates were incubated for about 48 hours at 37°C and 5 % CO_2.

Combinatorial treatment in PDGF

1 falcon with 2 mL ST and 1 eppendorf tube with 1 mL ST + 4 µL PDGF was prepared, of which 100 µL was added into the wells that should not be treated with any compound (see pipetting pattern: starvation, + 20 ng/mL PDGF). The single treatment of SFN and JQ1 was done as described above (only with other concentrations).

5 falcons with 4 mL ST + 16 µL PDGF and 10 µM, 5 µM, 2.5 µM, 1.25 µM and 0 µM of SFN were prepared. Of this solution, 500 µL were added into eppendorf tubes for each different concentration of JQ1 (=5 x 500 µL).
To prepare the stock solution of JQ1, 5 eppendorf tubes were prepared with the concentrations of 12.5 µM, 25 µM, 50 µM, 100 µM and 200 µM. 1 µL of the JQ1 stock

solutions were added into each eppendorf tube in which SFN was already dissolved.

100 µL of each solution of the eppendorf tube was added into 4 wells of the 96 well plate. The 96-well plates were incubated for about 48 hours at 37°C and 5 % CO_2.

a) Pipetting pattern for SFN treatment (96 well plate)

	0 µM SFN (DMSO only)	2.5 µM SFN	5 µM SFN	10 µM SFN	25 µM SFN	0 µM SFN	2.5 µM SFN	5 µM SFN	10 µM SFN	25 µM SFN	
	STARVATION					20 ng/mL PDGF					
	0 µM SFN	2.5 µM SFN	5 µM SFN	10 µM SFN	25 µM SFN						
	Growth Medium (10% Serum)										

b) Pipetting pattern for JQ1 treatment (96 well plate)

	0 µM JQ1	0.125 µM JQ1	0.25 µM JQ1	0.5 µM JQ1	1 µM JQ1	0 µM JQ1	0.125 µM JQ1	0.25 µM JQ1	0.5 µM JQ1	1 µM JQ1	
	STARVATION					20 ng/mL PDGF					
	0 µM JQ1	0.125 µM JQ1	0.25 µM JQ1	0.5 µM JQ1	1 µM JQ1						
	Growth Medium (10% Serum)										

c) Pipetting pattern for the combinatorial experiments in serum stimulated cells (96 well plate)

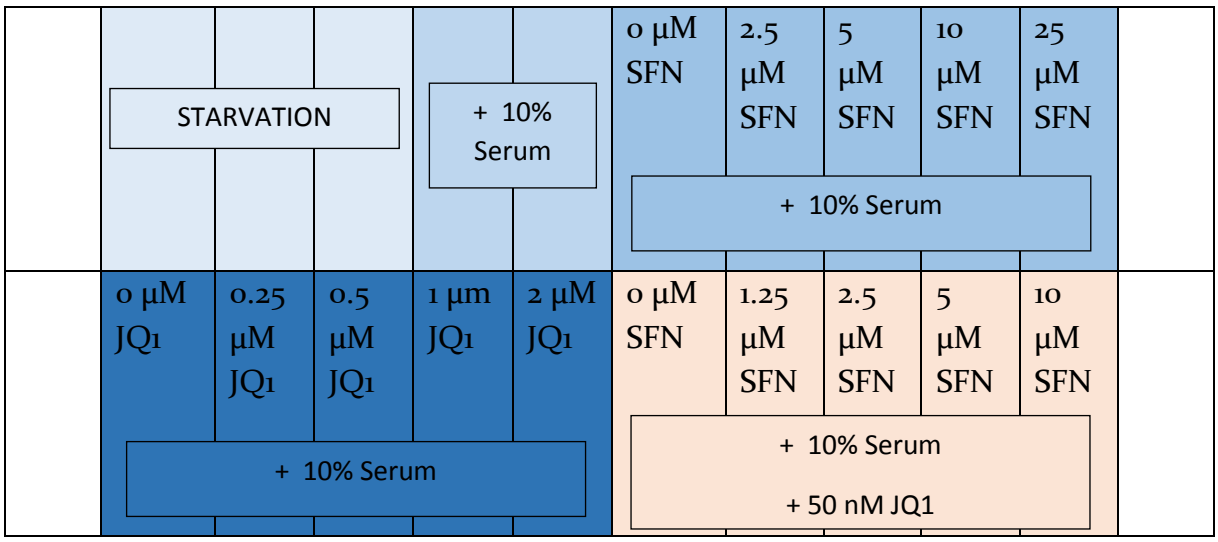

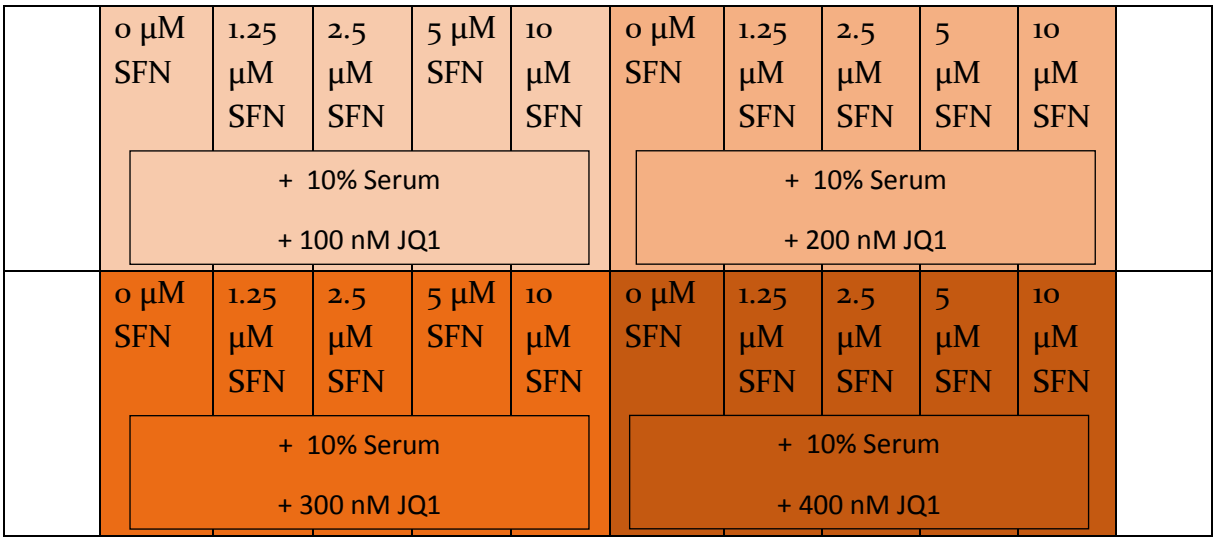

d) Pipetting pattern for the combinatorial experiments in PDGF stimulated cells (96 well plate)

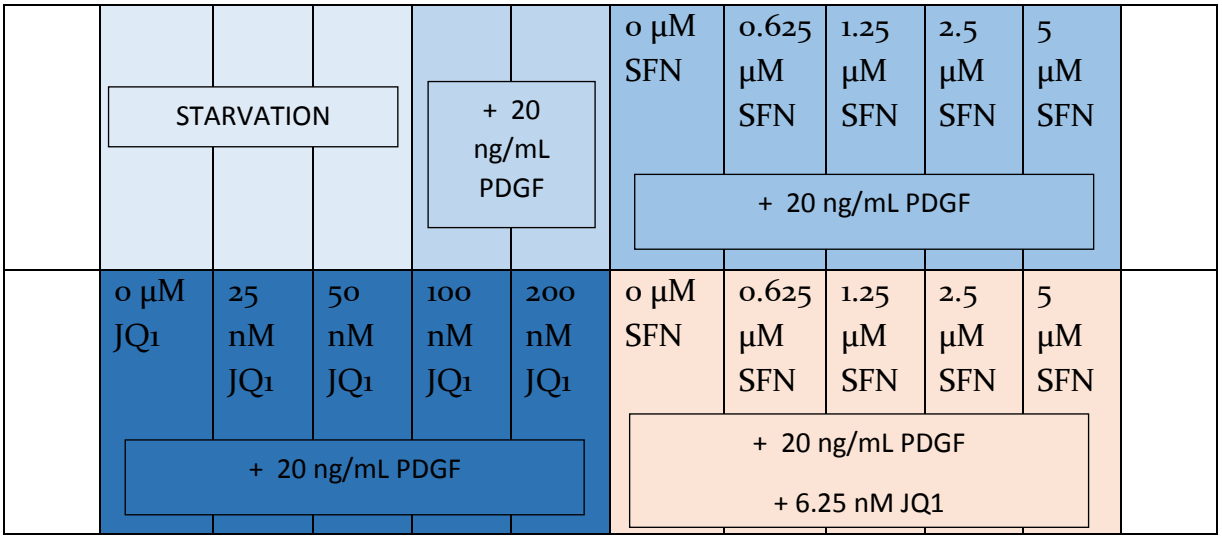

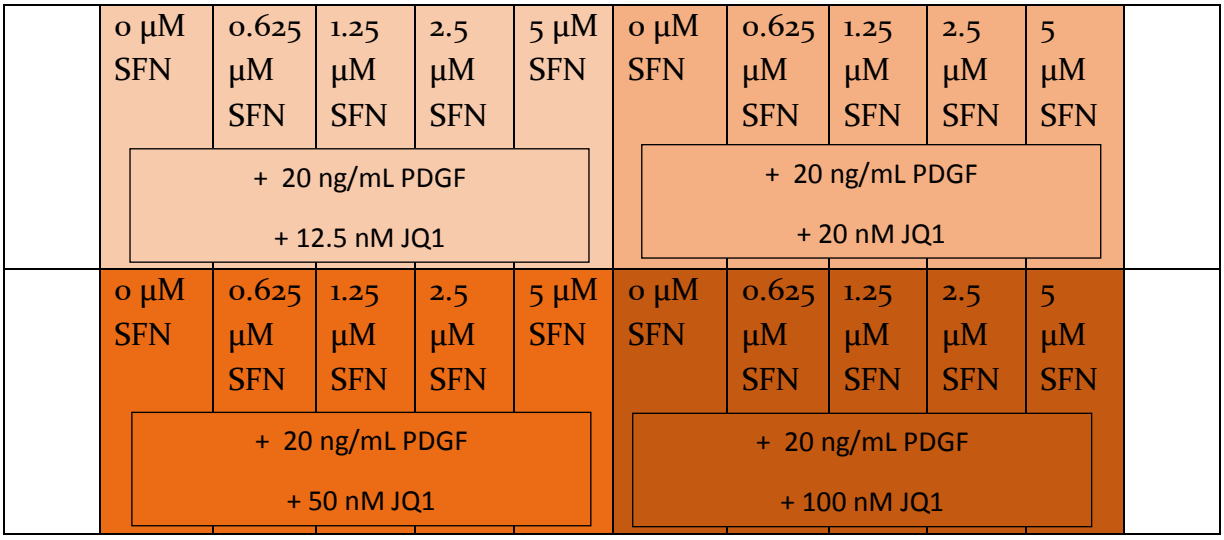

Crystal violet assay

After 48 hours of incubation, the medium was discarded and the wells were washed with 100 µL of PBS. 75 µL crystal violet solution was then added. After 3 – 5 minutes the crystal violet solution was discarded and the excessive dye was rinsed off with tap water. After drying at room temperature EtOH/Citrate solution (150 µl per well) was added in order to solubilize crystal violet. The biomass was quantified by spectrophotometry at 595 nm with the TECAN Sunrise™.

The measurement settings were:

Measurement mode	Absorbance
Measurement wavelength	595 nm
Read mode	Normal
Shake duration (Inside Normal)	10 sec
Shake settle time	3 sec

Evaluation

The mean values of serum and PDGF stimulated cells were subtracted from the mean values of starved cells. All treated cells were then normalized to cells that had no treatment (0 µM SFN/JQ1). IC50 values were determined by curve fitting of 5 different concentrations of the test compounds using GraphPad Prism 4 and GraphPad Prism 6.

For the combinatorial experiments, the IC50 of SFN with each different concentration of JQ1 was calculated and plotted into a isobologram. The X axis of the isobologram represents the different concentrations of JQ1 and the Y axis the different concentrations of SFN. The Y axis represents only the different concentrations of SFN, which means that the dot on the Y axis shows the IC50 of SFN alone without any JQ1 co-treatment (the same is valid in analogy for JQ1 and the X axis). The combinatorial index (CI) was calculated as CI = a/A + b/B, with a and b being the needed concentrations of compound A and B in combination to reach 50% inhibition and A

and B are the IC50 of the active compounds when applied alone. CI < 1 indicates synergy, CI > 1 indicates antagonism and CI = 1 indicates an additive effect of the two compounds with respect to the assayed readout/bioactivity.

c) Flow cytometric cell cycle analysis

Introduction

Flow cytometry is commonly used to analyse the size, granularity and fluorescence of cells in a cell population. Therefore, cells need to be in suspension in order to pass one by one across a laser beam in the flow cytometer. The forward scattered light of the cells correlates with their size and the sideward scattered light correlates with granularity and also size. Different fluoresence detectors are able to measure the fluorescence intensity if cells are dyed with a fluorophor, e.g. propidium iodide (PI) (Picot et al., 2012).

Preparation

5 million cells were seeded in ten 6 cm dishes. Each dish contained 3 mL of growth medium with 500 000 cells. On the next day the cells were washed with PBS and 3 mL of starvation medium was added. The cells were starved for 24 hours.

Treatment

a) Time course experiment

DISH	WEDNESDAY	THURSDAY	SAMPLE
#1	08:00 HARVEST**		Control 1
#2	08:00 Serum * 12:00 HARVEST		Serum 4 hrs
#3	08:00 PDGF * 12:00 HARVEST		PDGF 4 hrs
#4	08:00 Serum 16:00 HARVEST		Serum 8 hrs
#5	08:00 PDGF 16:00 HARVEST		PDGF 8 hrs
#6	08:00 Serum	08:00 HARVEST	Serum 24 hrs
#7	08:00 PDGF	08:00 HARVEST	PDGF 24 hrs
#8	16:00 HARVEST		Control 2
#9	16:00 Serum	08:00 HARVEST	Serum 16 hrs
#10	16:00 PDGF	08:00 HARVEST	PDGF 16 hrs

*For addition of serum / PDGF: The medium was removed, fresh starvation medium (3 mL) was added and then 300 µL FBS or 6 µL PDGF was added.

**HARVEST: The cells were washed with PBS and detached with 2 mL Trypsin. 1.5 mL GM was added and the cell suspensions were collected in ten FACS tubes. After four minutes of centrifugation (1400 rotations / min; 372,5 x g) the cells were washed again with PBS and the pellet was taken up in 300 µL Propidium iodide solution. The samples were stored in the dark at 4°C.

b) Treatment with SFN (6 cm dishes) for 24 hours

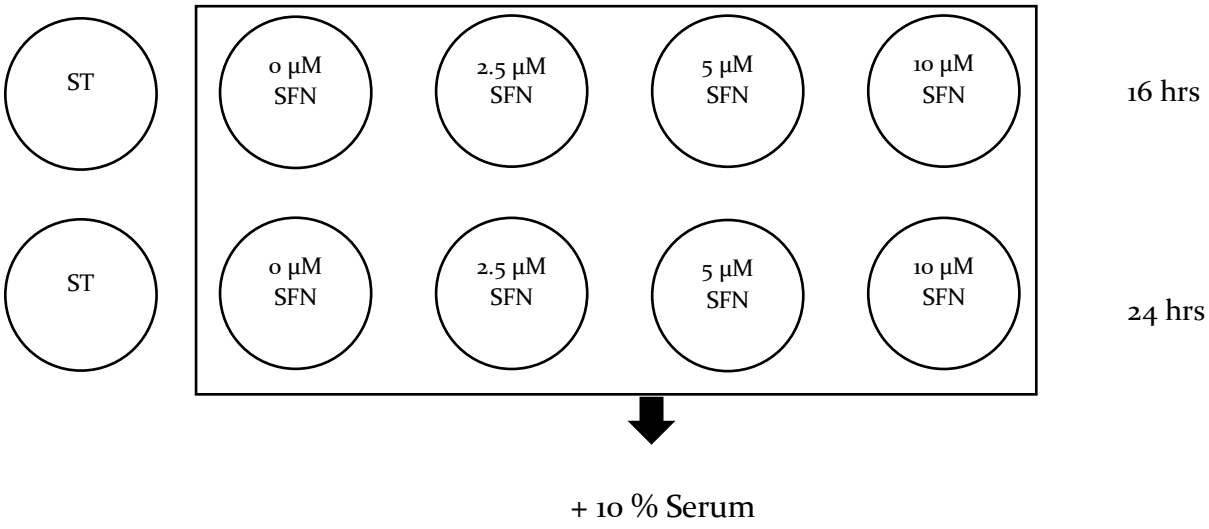

c) Treatment with JQ1 (6 cm dishes) for 24 hours

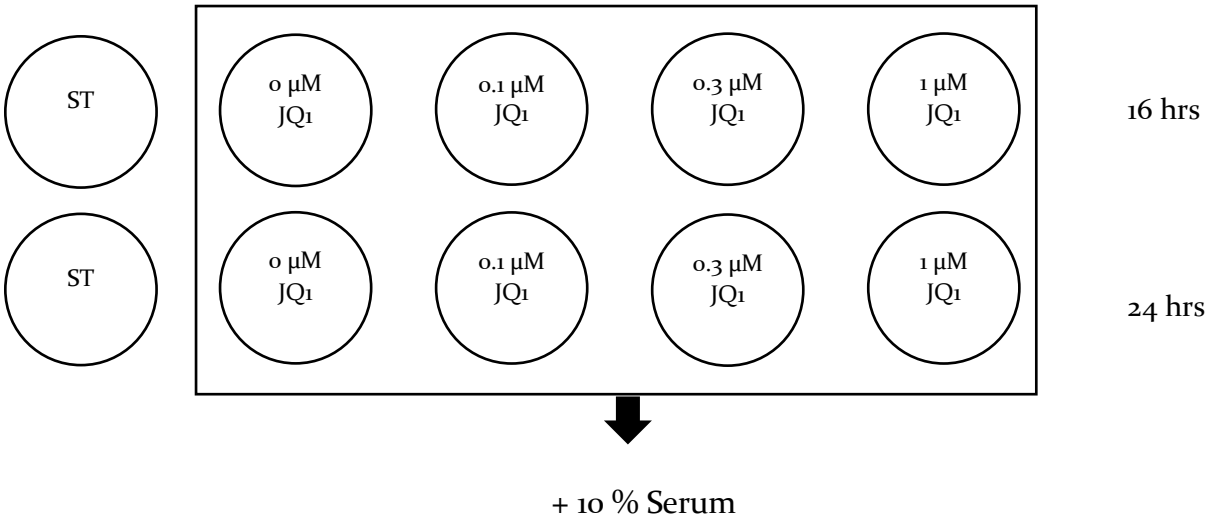

For addition of Serum and HARVEST see Time course experiment.

Analysis

After collecting the cell pellets in 300 µL Propidium iodide the samples were vortexed and measured with FACSCalibur™ in the FL2-A channel. BD CellQuest™ Pro Software

was used to analyze the data. The cell cycle phases were marked on the histogram plot (**Fig.8**) and the area under the curve (amount of cells) for each cell cycle phase was read out of the histogram statistics. The amount of cells for each phase was illustrated using GraphPad Prism 4 and 6.

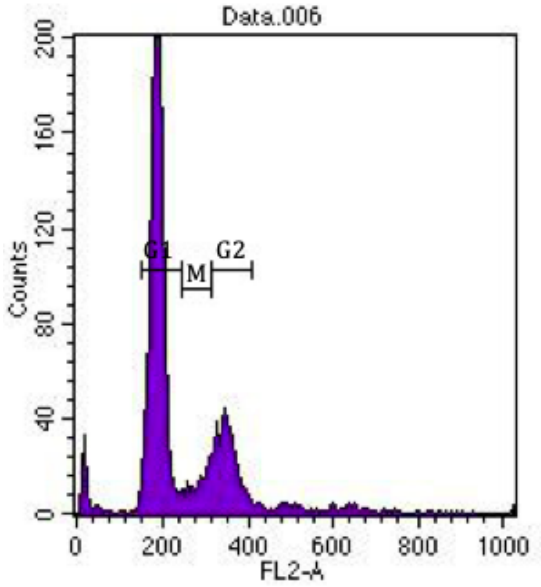

Fig. 8 **Example of a histogram plot.** Starved VSMC were incubated 24 hours with the compounds before stained with PI. Cell cycle analysis was performed by Flow cytometry. The graph shows the cell count in the different cell cycle phases, which correlates to the propidium iodide intensity (Fluorescence 2 - Area).

d) Western blotting

Preparation

The cells were seeded on 6-well plates, containing 1 million cells (=166 666 cells per well). Each well contained 2 mL of growth medium. For two experiments, 6 cm dishes were used. In this case, each dish contained 300 000 cells in 3 mL of growth medium.

On the next day 2 mL of starvation medium (3 mL for the 6 cm dishes) was added to the wells after discarding the growth medium.

Treatment

The treatment of the cells was performed after 24 hours of starvation. The compounds were dissolved in ST for one 6 - well plate. For the second plate, 200 µL FBS was added to each well (= 10% Serum). The cells were treated for 24 hours.

Pipetting pattern for western blotting (6 well plate) - combinatorial treatment

DMSO	SFN IC50 2.860 µM	JQ1 IC50 231 nM
SFN 3.5 µM + JQ1 50 nM	SFN 3.5 µM + JQ1 50 nM	SFN IC50 2.860 µM + JQ1 IC50 231 nM

(= concentration, which showed highest antagonistic effect in the crystal violet assay)

Protein Extraction

The plates were kept on ice during the whole procedure. First, the medium was removed and the cells were washed twice with cold PBS (2 mL for each well). After removing PBS completely, 50 µL of lysis buffer (70 µL for two experiments with the 6 cm dishes) was added. The lysis buffer contains not only detergents to open up the cells, but also protease inhibitors to stop the proteolytic activity of proteases in the lysosomes of the cells. After 5 minutes of incubation, the cells were scraped off with a clean cell-scraper and transferred into a 1.5 mL eppendorf tube. To complete the cell lysis the collected cells were sonificated for 5 seconds. After 15 minutes of centrifugation (13.000 rotations per minute (rpm); 16060 x g) at 4°C 5 µL of the supernatants were added into a new Eppendorf tube with 45 µL Aqua bidestillata (1:10 dilution).

Bradford Assay

The Bradford Assay is used to measure the protein content of samples. The dye Coomassie Brilliant Blue is able to bind to amino acids, which results in a shift in the absorbance maximum to 595nm, which can be measured with a spectrophotometer. 10 µL of the prepared dilutions were added as triplicates in three wells of a 96-well plate. 7 different concentrations of bovine serum albumin (BSA) were pipetted as triplicates into the wells to create a standard curve. Afterwards, 190 µL of Bradford reagent was added. The absorption was measured with TECAN Sunrise™ after 5 minutes of incubation. The protein content was calculated using Excel.

SDS PAGE

Sodium dodecyl sulfat polyacrylamid gel electrophoresis (SDS-PAGE) is commonly used to separate proteins according to their mass. It is based on the migration of proteins through a polyacrylamide gel within an electric field. It is important to denature the proteins and cover their intrinsic charge with SDS so that the migration through the gel is only dependent on the proteins' size.

Preparation of the gel

First, the separation gel was pipetted between two fixed glass plates and covered with isopropanol. The gel needs 30 to 60 minutes to polymerize. After polymerization the isopropanol was removed and the stacking gel was added. The comb was wiped with EtOH and placed on top of the gel. When the stacking gel was polymerized the gel was stored at 4°C in a wet pulp in a plastic bag.

SDS PAGE

To perform the SDS Page the glass plates were fixed with an apparatus and placed into a chamber (**Fig. 9**) . Then the chamber was filled with electrophoresis buffer. After removing the comb the slots were rinsed with electrophoresis buffer and the gel could finally be loaded with the desired volume of proteins. 2 µg of protein for the first experiment, 2.8 µg for the second and 3.5 µg of protein for the third experiment was loaded per lane. The first slot was filled with 10 – 15 µl of marker (Precision Plus Protein™ Standards). The current was set to 20 mA per gel. The SDS PAGE is finished when the blue frontage reaches the lower end of the plate.

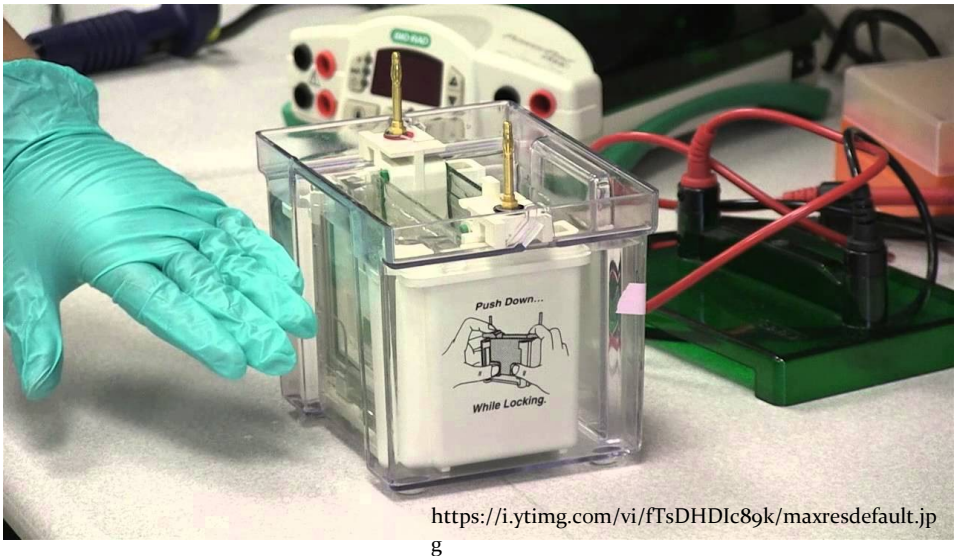

https://i.ytimg.com/vi/fTsDHDIc89k/maxresdefault.jpg

Fig. 9 **Preparation for the SDS Page.** The "push down while lock" apparatus fixes the glass plates and has the connectors for the power supply.

Blotting

To be able to detect the proteins with antibodies it is necessary to transfer the separated proteins from the gel matrix onto a polyvinylidene fluoride (PVDF) membrane. Therefore, after activating the membrane for one minute in methanol, it was transferred to blotting buffer and placed on the gel between two filter papers and fiber pads (**Fig. 10**). The 'blotting sandwiches' were placed into the blotting tank, which was filled with blotting buffer and placed on a magnetic stirrer. A box with frozen buffer was also placed in order to cool the chamber. Voltage was applied at 100V for 100 minutes.

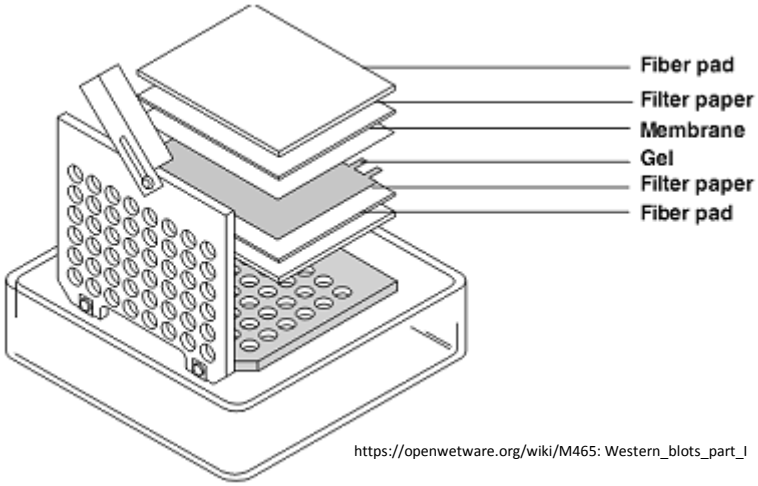

Fig. 10 **Assembly of a sandwich in Western Blot.**

Blocking

In order to block unspecific binding sites the membrane was incubated with 5% BSA (25 ml per membrane) on a rocking platform. Then, after washing three times with TBST, the membrane was put in 5 mL primary antibody solution for two hours on a rotator at room temperature. This step can also be performed overnight at 4°C on a rotator.
After washing three times with TBST for 15 minutes the membrane was transferred into the falcons with the secondary antibodies and incubated for 2 hours at room temperature on a rotator. Then, again after washing three times with TBST, the membrane was incubated with ECL detection solution for one minute. The detection was performed with Image Reader LAS-3000™. The intensities of the bands (densitometry) were determined with the use of the Multi Gauge V3.0 software and corrected for the background signal. The values were put in an Excel file and the values of the protein of interest were divided by the values of the loading control (actin or tubulin). The bar graphs of compiled analyses were represented in GraphPad Prism 4 and 6.

In order to incubate one membrane sequentially with different primary antibodies the membrane had to be stripped. For this, it was washed again for 5 - 10 minutes with TBST and for 15 minutes with 0.5 N NaOH. Then, after washing again for 5 – 10 minutes with TBST, the membrane is ready for another incubation.

C) Results and Discussion

1) Proliferation of VSMC

Cell cycle progression of VSMC

To monitor cell cycle progression of VSMC over time, we used the Flow cytometric analysis of PI stained cells after cell stimulation with serum or PDGF for different periods of time.

The results showed that 16 hours after mitogenic stimulation the number of cells in the S and G2 phases increase and the G1 phase decreases. Therefore we decided to compare the potential antiproliferative effects of the test compounds on VSMC after 16 and 24 hours in order to find out how the active compounds may influence the cell cycle progression (**Fig. 11**).

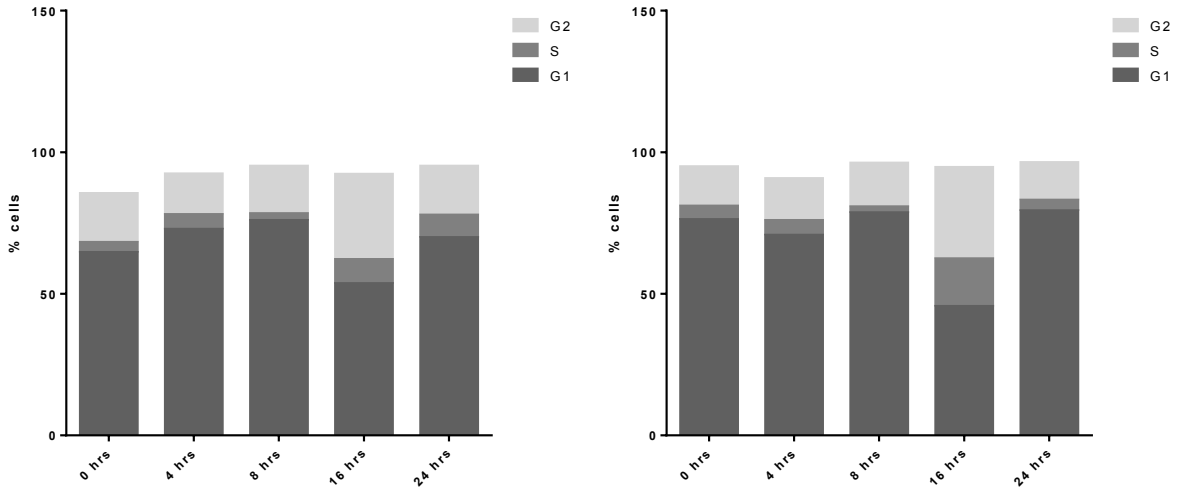

Fig.11 **Cell cycle progression of serum (left) and PDGF (right) stimulated VSMC**. Cells were starved for 24 hours and stimulated with either serum (+10 %) or PDGF (20 ng/mL) for four, six, eight, sixteen and twenty-four hours and then harvested by trypsinization. PI was used to dye the DNA of the cells in order to determine the percentage of cells with the flow cytometer. Results are taken from one biological experiment.

Proliferation of serum- and PDGF-activated VSMC

In a next step we aimed to compare the extent of VSMC proliferation induced by PDGF (potent physiological mitogen for VSMC) and serum. Therefore we stimulated starved VSMC with serum or PDGF and assessed biomass after 48 hours with the crystal violet assay.

The results showed that VSMC proliferate (increase biomass) upon serum or PDGF stimulation, with a reproducibly stronger effect in serum than in PDGF since serum contains lots of mitogenic compounds, such as growth factors and serum proteins, which are essential for the cells' growth (**Fig. 12**).

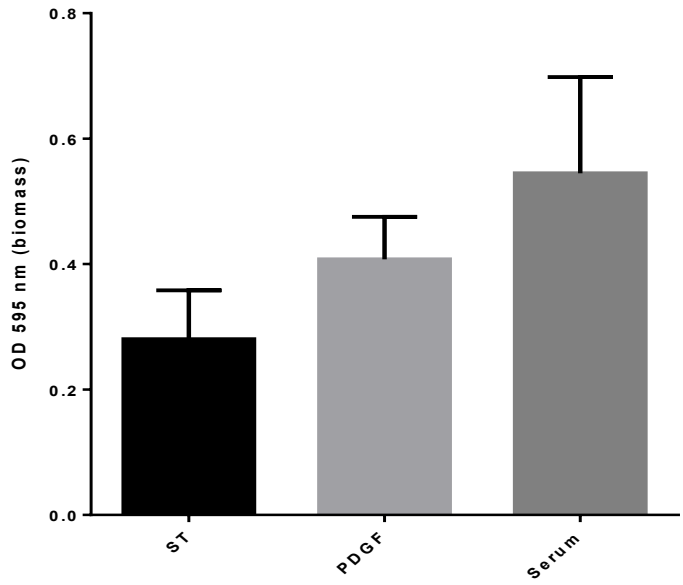

Fig. 12 **Proliferation of activated VSMC.** The cells were stimulated with serum (+10%) or PDGF (20 ng/mL) after 24 hours of starvation. Cell proliferation was assessed with crystal violet assay after 48 hours of stimulation. The Y axis represents the optical density (OD) of dissolved crystal violet at 595 nm. Results are shown as means ± standard deviation (SD) of six independent experiments.

2) Influence of Sulforaphane on VSMC Proliferation

To investigate the effect of Sulforaphane on VSMC proliferation, we treated activated VSMC with different concentrations of Sulforaphane and assesed proliferation with the crystal violet assay. In addition, we examined the cell cycle distribution with the flow cytometer in order to find out in which cell cycle phase SFN arrests the cells.

The results showed that the treatment of SFN inhibits the proliferation of VSMC, with a stronger effect on PDGF than on serum-induced proliferation (**Fig. 13**). It was expected that proliferation in serum is more difficult to inhibit since the serum has lots of growth factors that stimulate the cells by multiple pathways to divide. The IC50 for SFN were 5.05 µM for serum stimulated VSMC and 1.39 µM for PDGF stimulated VSMC, respectively (**Fig. 14**).

Cell cycle analysis showed that SFN leads to a G1 – arrest in VSMC after 16 and 24 hours of PDGF stimulation (**Fig. 15**). The higher percentage of cells in the G1 phase shows that SFN arrests at the G1 phase and stops VSMC proliferation, which goes along with a lower percentage of cells in the S – phase.
If the G2 phase increased after 16 hours or after 24 hours, than it would mean that SFN arrested at the G2 phase or simply slowed down the progression through cell cycle. Since the G2 phase does not increase after 16 hours or 24 hours, there is likely no G2 arrest or retarded cell cycle progression with the treatment of SFN.

Previous studies have already reported that SFN inhibits the PDGF-induced VSMC proliferation (at the concentrations 0.5 µM, 1 µM and 2 µM) by arresting them at the G1/S phase through the up-upregulation of the tumor suppressor p53 and the kinase inhibitor p21 (Shawky and Segar, 2017). Therefore, our IC50 for SFN in PDGF stimulated VSMC (1.39 µM) and apparent G1 arrest are consistent with the results of Shawky and Segar.

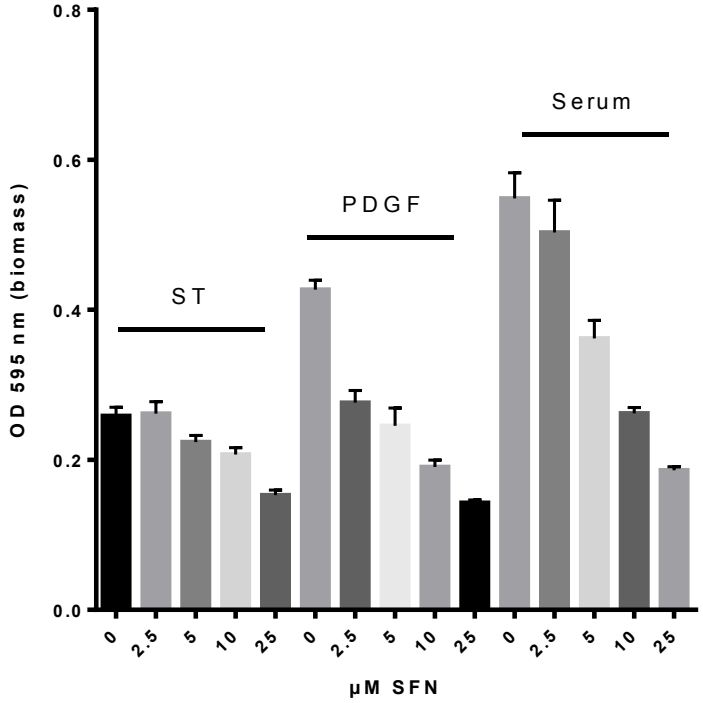

Fig. 13 **Sulforaphane inhibits Serum and PDGF-induced VSMC proliferation concentration-dependently**. After 24 hours of starvation, VSMC were treated with different concentrations of SFN and stimulated with either serum (+10 %) or PDGF (20 ng/mL). Biomass (OD 595 nm) was assessed by crystal violet assay after 48 hours of incubation. Results are shown as means ± SD of three independent experiments.

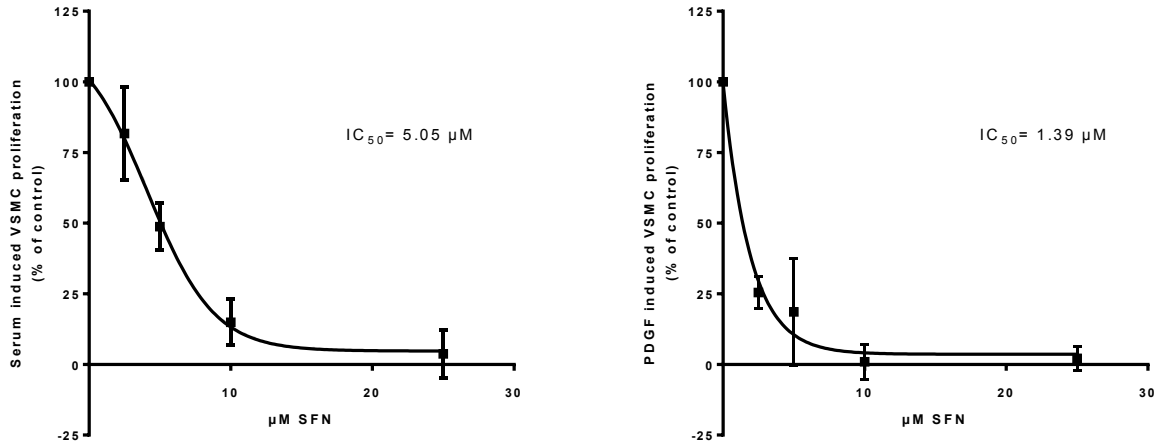

Fig. 14 **Dose – response curves of SFN for serum (left) and PDGF (right) stimulated VSMC.** After 24 hours of starvation, VSMC were treated with different concentrations of SFN and stimulated with either serum (+10 %) or PDGF (20 ng/mL). Cell proliferation was asessed by crystal violet assay after 48 hours. Results are shown as means ± SD of three (left) and two (right) independent experiments.

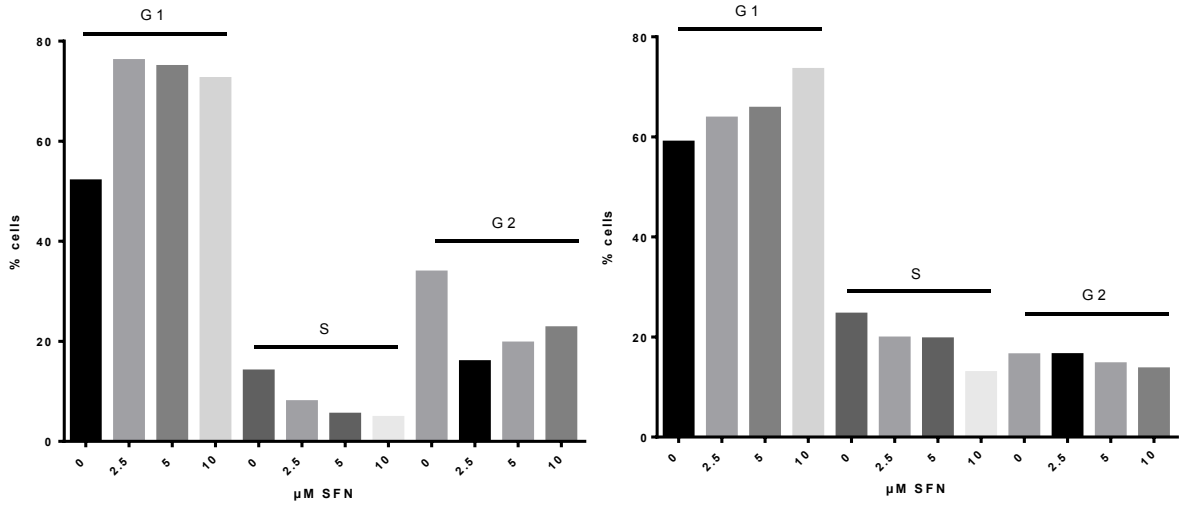

Fig. 15 **Sulforaphane inhibits VSMC proliferation at the G1 phase.** Cell cycle distribution of SFN treated and serum (+10 %) stimulated VSMC after 16 hours (left) and 24 hours (right). Starved VSMC were treated with serum and with different concentrations of SFN for 48 hours and harvested by trypsinization. PI was used to stain the DNA of the cells. Cell cycle distribution was measured by flow cytometry. The results are taken from one biological experiment.

3) Influence of JQ1 on VSMC Proliferation

To investigate the effect of JQ1 on VSMC proliferation, we treated activated VSMC with different concentrations of JQ1 and assesed proliferation with the crystal violet assay. In addition, we examined the cell cycle distribution with the flow cytometer.

Fig. 16 shows that the proliferation of VSMC is hindered by the treatment of JQ1 in a concentration dependent manner. JQ1 seems to be more potent compared to SFN since the IC50 in serum stimulated VSMC lies at 889 nM (**Fig. 17**). The IC50 of only 102 nM for PDGF stimulated cells qualifies JQ1 as a very potent antiproliferative compound that is already being researched in clinical trials (Arshad et al., 2016).

Wang et al. (2015) already showed that JQ1 inhibited PDGF-induced rat aortic smooth muscle cell proliferation in a dose dependent manner throughout a range of concentrations of 5 nM to 10 µM, which is compatible with our results (IC50 102 nM).

As with SFN, JQ1 leads to a G1 cell cycle arrest in activated VSMC. The percentage of cells in G1 phase increases dose-dependently (**Fig. 18**), as particularly evident after 16 hours. In chondrosarcoma cells JQ1 is reported to arrest cell cycle at the G1 phase by the up-regulation of the cycline-dependent kinase (CDK) inhibitors p21 and p27 (Zhang et al., 2017), suggesting a general cell-type unrelated antiproliferative activity.

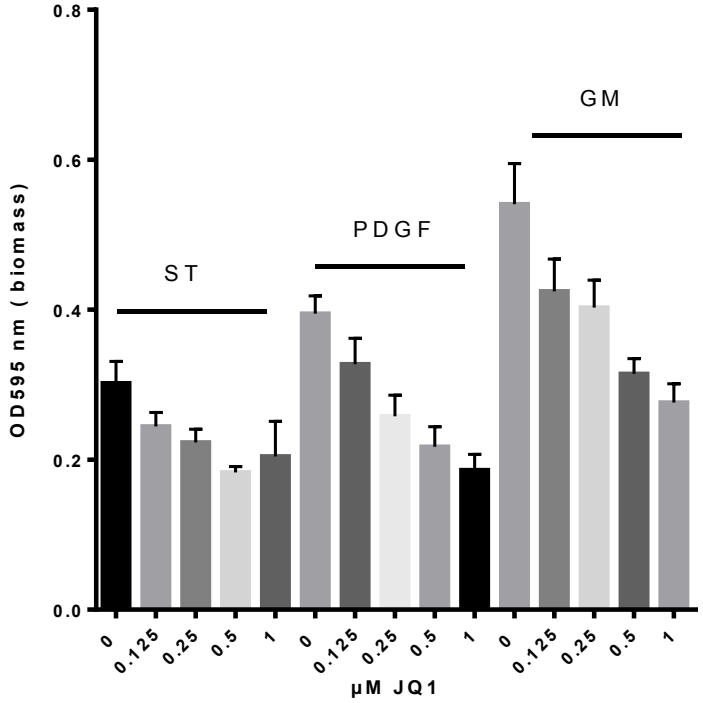

Fig. 16 **JQ1 inhibits serum and PDGF induced VSMC proliferation concentration- dependently.** After 24 hours of starvation, VSMC were treated with different concentrations of JQ1 and stimulated with either serum (+10 %) or PDGF (20 ng/mL). Biomass (OD595 nm) was assessed by crystal violet assay after 48 hours of incubation. Results are shown as means ± SD of three independent experiments.

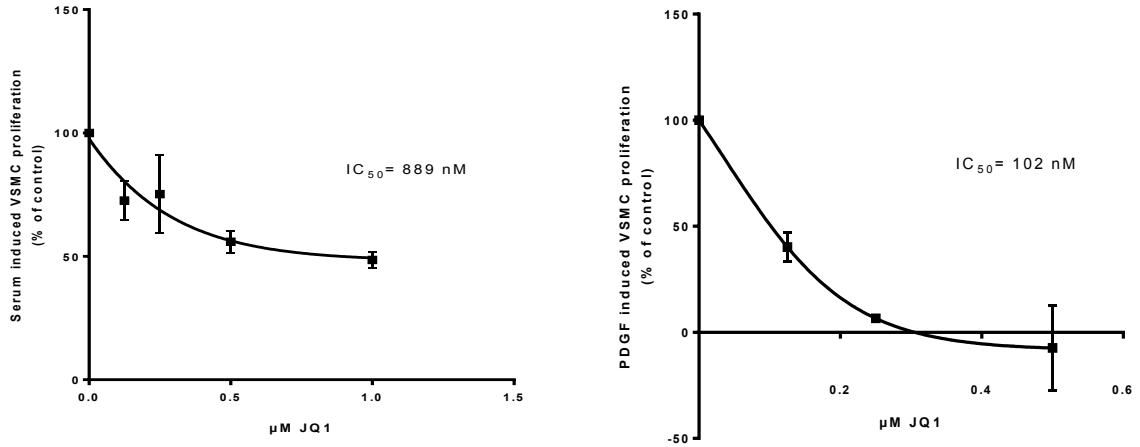

Fig. 17 **Dose – response curves of JQ1 for serum (left) and PDGF (right) stimulated VSMC.** After 24 hours of starvation, VSMC were treated with different concentrations of JQ1 and stimulated with either serum (+10 %) or PDGF (20 ng/mL). Cell proliferation was assessed by crystal violet assay after 48 hours. Results are shown as means ± SD of three (left) and two (right) independent experiments.

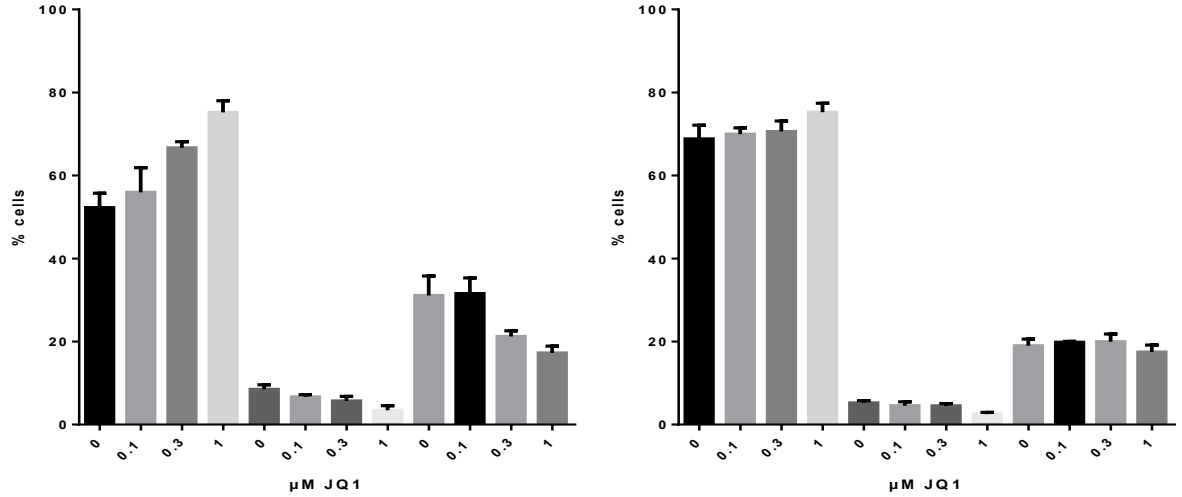

Fig. 18 **JQ1 inhibits VSMC proliferation at the G1 phase.** Cell cycle distribution of JQ1 treated and serum (+10 %) stimulated VSMC after 16 hours (left) and 24 hours (right). Starved VSMC were treated with serum and with different concentrations of JQ1 for 48 hours and harvested by trypsinization. PI was used to stain the DNA of the cells. Cell cycle distribution was measured by flow cytometry. Results are shown as means ± SD of three independent experiments.

4) Combinatorial treatment of VSMC with Sulforaphane and JQ1

The combinatorial treatment with SFN and JQ1 in VSMC was not investigated so far. Such combinatorial treatment regimens optimally might maximize the effect by synergy and minimize potential harmful side effects by using lower doses of the single compounds. Therefore, we combined SFN and JQ1 in different concentrations in activated VSMC and assessed proliferation by crystal violet assay to see the influence of the combinatorial treatment on VSMC proliferation and to appreciate potential antagonistic, additive or synergistic effects.

The combination of both compounds in serum as well as in PDGF stimulated VSMC showed an antagonistic effect in all experiments assessing cell proliferation (**Fig. 19**). The combinatorial indexes (CI), calculated to reach growth inhibition by 50%, increased with higher concentrations of JQ1 (**Table 1**). However, despite this unexpected and rather decouraging result regarding proliferating VSMC, it will still be of importance to investigate how the combinatorial treatment with SFN and JQ1 will behave in vivo models, or at least in VSMC co-cultured with endothelial cells and macrophages. It may well be that the combination of SFN and JQ1 could still lead to a synergistic anti-atherogenic effect in an entire organism by enhanced inhibition of proatherogenic processes coming from different cell types, including inflammatory signals from immune cells or endothelial dysfunction.

50 % Inhibition (Serum)		
Conc. JQ1	Conc. SFN	CI
0 nM	2.9 µM	n.a.
50 nM	3.5 µM	1.42
100 nM	3.1 µM	1.50
200 nM	3.3 µM	2.0
231 nM	0 µM	n.a.

50 % Inhibition (PDGF)		
Conc. JQ1	Conc. SFN	CI
0 nM	1.2 µM	n.a.
6.25 nM	1.4 µM	1.27
12.5 nM	1.7 µM	1.61
25 nM	1.4 µM	1.56
50 nM	1.2 µM	1.79
63.5 nM	0 µM	n.a.

Table 1 **Combinatorial indexes for SFN and JQ1 in serum (+10%) and PDGF (20 ng/mL) stimulated VSMC.** The table shows the concentrations of SFN and JQ1 that were needed to reach a 50% inhibition of VSMC proliferation. The combinatorial index (CI) was calculated as CI = a/A + b/B, with a and b being the needed concentrations of compound A and B in combination to reach 50% inhibition and A and B are the IC50 of the active compounds when applied alone. CI < 1 indicates synergy, CI > 1 indicates antagonism and CI = 1 indicates an additive effect. Results are taken from three indepenent biological experiments.

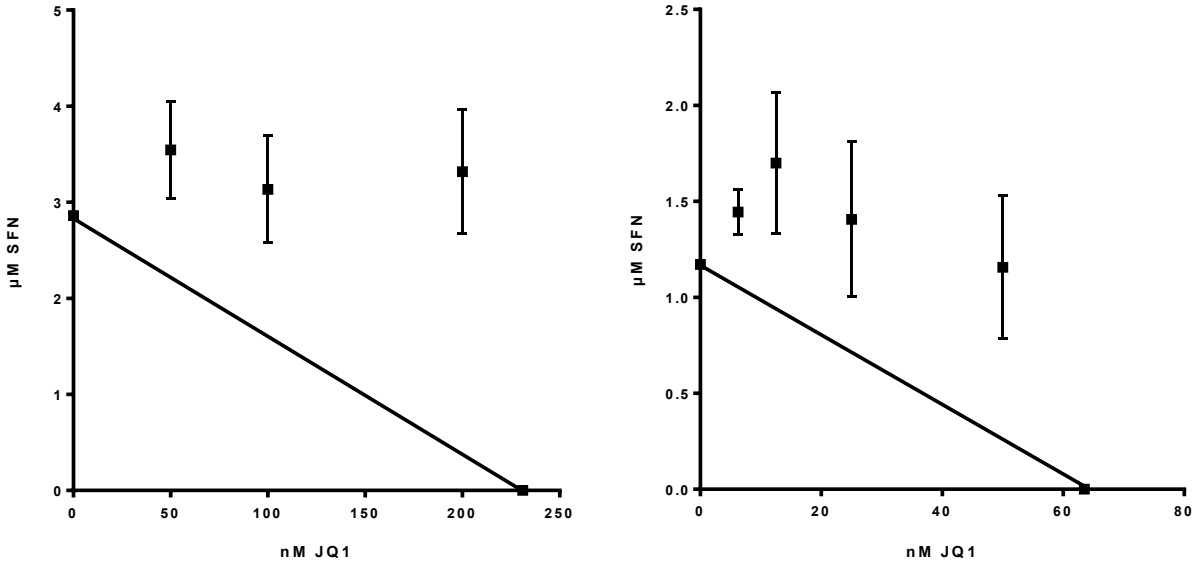

Fig. 19 **SFN and JQ1 show an antagonistic effect on VSMC proliferation.** The isobologram of serum (left) and PDGF (right) stimulated VSMC shows an antagonistic effect of the combinatorial treatment of SFN and JQ on VSMC proliferation. VSMC were starved for 24 hours, stimulated with either serum (+10 %) or PDGF (20 ng/mL) and treated with different concentrations of Sulforaphane and JQ1 for 48 hours. The dots represent the IC50 concentrations of SFN when combined with JQ1. Dots under the line would show a synergistic effect, the dots on the line show an additive effect and the dots above the line show an antagonistic effect. The dots on the X/Y axis represents the IC50 of JQ1/SFN alone. Results are shown as means ± SD of three independent experiments.

5) Effects of Sulforaphane and JQ1 alone and in combination on Nrf2 target genes, BRD4 and PDGF-R

To gain a first insight into the antagonistic effect of SFN and JQ1 on VSMC proliferation, we treated activated VSMC with SFN and JQ1 alone and in combination in order to quantify the Nrf2 target proteins GCLC and HO-1, as well as BRD4 and PDGFR levels by the western blotting technique. Protein concentrations of BRD4, PDGFR and the Nrf2 target proteins GCLC and HO-1 was not examined before in VSMC upon combinatorial treatment with SFN and JQ1. However, Chatterjee et al. (2016) showed that JQ1 enhances the expression of several Nrf2 target genes together with Oltipraz (a Keap1-inhibitor) and the Nrf2 target gene NQO1 together with Sulforaphane in HEK293 cells.

HO-1 & GCLC

Our results showed that the Nrf2 target genes **HO-1** and **GCLC** are both induced by SFN and JQ1, as seen in increased protein abundance in the immunoblots. Notably though, the combination of SFN and JQ1 does not show an antagonistic, but rather an additive or even synergistic effect, with a stronger effect in GCLC than in HO-1 expression (**Fig. 20**, **Fig. 21**). The positive cooperativity regarding the Nrf2 gene expression is in line with previous reports showing that BRD4 inhibitors positively influence Nrf2 signaling by preventing the BRD4 - Nrf2 interaction. Interestingly, the enhanced activation of Nrf2 signaling did not result in enhanced VSMC proliferation inhibition, as seen in the previous proliferation assays. There could be several **reasons**

why the enhanced Nrf2 activation after BRD4 inhibition did not lead to enhanced VSMC proliferation inhibition by SFN and JQ1 combinations:

a) SFN could inhibit VSMC proliferation Nrf2-independently. Therefore, a higher level of Nrf2 target genes together with JQ1 did not lead to an enhanced inhibition of VSMC proliferation. This would confirm to the recent results of Shawky and Segar, which suggested that the activation of the Nrf2 pathway by Sulforaphane plays a minor role in VSMC proliferation. An experiment in Nrf2-deficient VSMC could address the question, to what extent SFN inhibits VSMC proliferation via Nrf2 activation.

b) JQ1 could lose its anti-proliferative activity over time by being ejected from the cell by the detoxification mechanisms triggered by Nrf2. This is quite possible since Sulforaphane is reported to increase the expression of the multidrug transporter multidrug resistance-associated protein 2 (MRP2) in primary hepatocytes, which is able to actively pump drugs out of the cells (Payen et al., 2001). Therefore, it will be of interest to study the expression of multidrug transporters upon single and combinatorial treatment with SFN and JQ1 in VSMC in order to find out if expression of the transporters are enhanced upon combinatorial treatment compared to single treatment.

c) The different modes of inhibition employed by SFN and JQ1 could counteract each other. For example, on an epigenetic level, SFN-induced histone acetylation could lead to new interaction sites for BET-proteins that are not sensitive to JQ1. BET-proteins may bind to SFN-induced new acetylation sites on histones and contribute to the phenotype switch of VSMC to a proliferative state.

Several previous studies have reported that compounds such as curcumin, sulfasalazin, trans-resveratrol and dimethylfumarate inhibit VSMC proliferation through Nrf2-induced HO-1 expression (Shawky and Segar, 2017). Therefore, it appears somewhat contradictory that increased HO-1 expression after combinatorial treatment with SFN and JQ1 does not lead to enhanced but diminished inhibition of VSMC proliferation. Further investigations are required to find out whether Nrf2 signaling and HO-1 expression is sufficient to inhibit VSMC proliferation or if the reported compounds

may also be able to inhibit VSMC proliferation by other or additional means than activating Nrf2, which is the case for Sulforaphane.

BRD4 & PDGFR

BRD4 was found to be upregulated in activated VSMC (Wang et al., 2015). Its concentrations were not investigated so far in VSMC upon JQ1 or SFN treatment. BRD4 levels could be altered by JQ1 or SFN presumably through epigenetic mechanisms, since neither SFN nor JQ1 could influence its protein expression (at the current status of knowledge) except by epigenetic regulations.

With regards to BRD4 and PDGFR abundance, our obtained western blot data show a big standard deviation between the individual experiments and rather suggest that both proteins are not markedly affected by the treatment with SFN and JQ1. For PDGFR, there might be a tendency that serum activated cells express higher levels which are lowered by SFN and the combination of SFN and JQ1. SFN is reported to not alter PDGFRβ levels (Yoo et al., 2013), however, it will be of importance to further investigate whether SFN will alter PDGFRα levels since the PDGFRα is a prominent player in SMC proliferation.

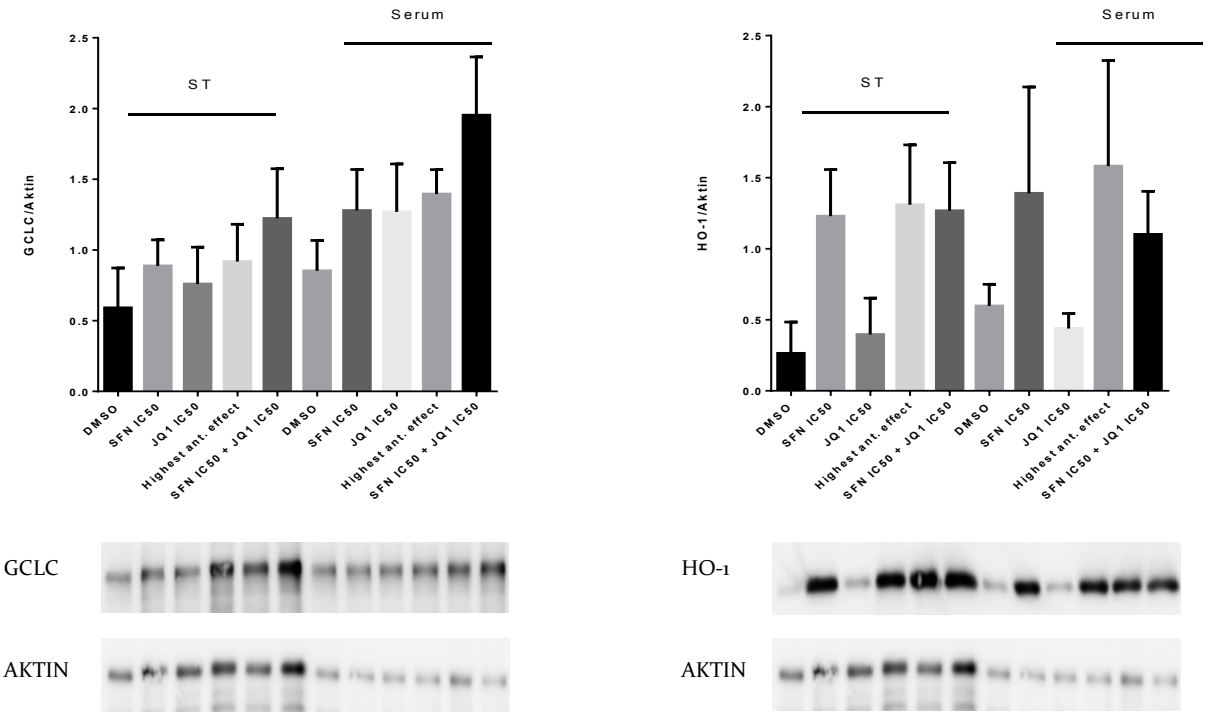

Fig. 20 **Effect of SFN and JQ1 (alone and in combination) on GCLC (left) and HO-1 (right) levels.** VSMC were starved for 24 hours. The cells were treated for 24 hours with DMSO, SFN IC50 (2.860 µM), JQ1 IC50 (231 nM), twice with the concentration that showed the highest antagonistic effect (SFN 3.5 µM + JQ1 50 nM) and with IC50 of both compounds and then lysed. The expression of GCLC and HO-1 was analysed by western blot, as shown in representative pictures. Actin was processed in parallel as a loading control. Densitometric results are shown as means ± SD of three independent experiments.

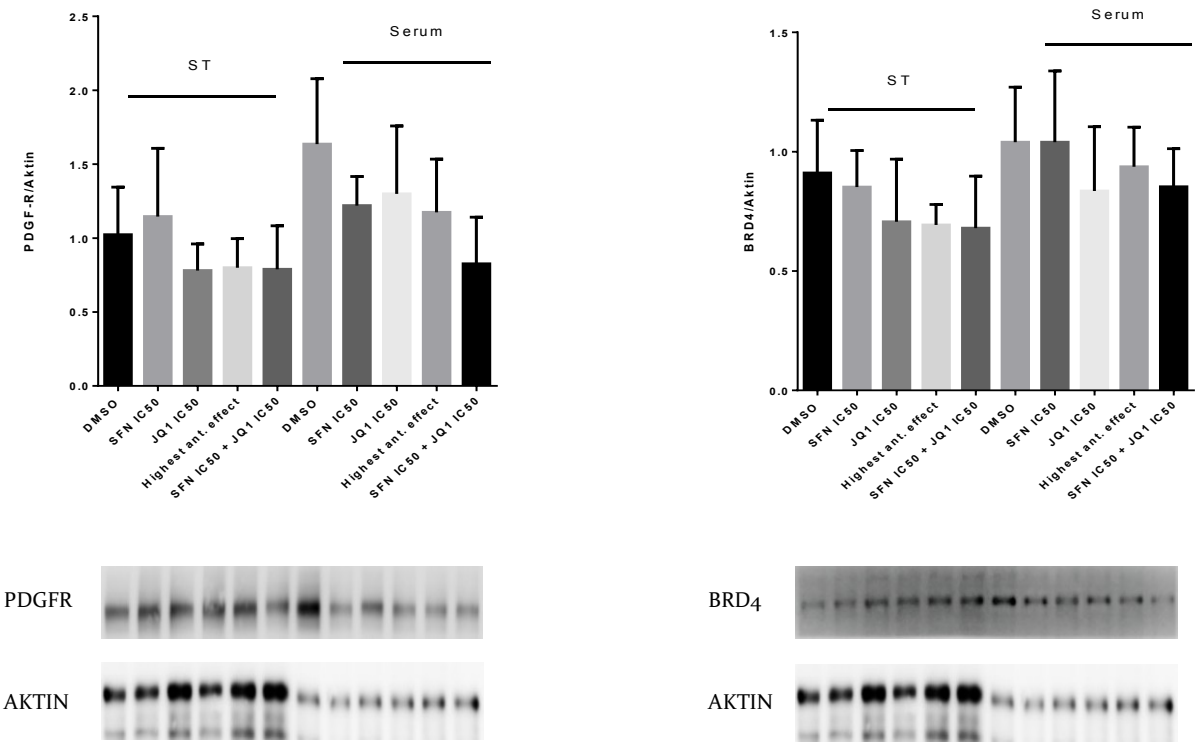

Fig. 21 **Effect of SFN and JQ1 (alone and in combination) on PDGFR (left) and BRD4 (right) levels**. VSMC were starved for 24 hours. The cells were treated for 24 hours with DMSO, SFN IC50 (2.860 µM), JQ1 IC50 (231 nM), twice with the concentration that showed the highest antagonistic effect (SFN 3.5 µM + JQ1 50 nM) and with IC50 of both compounds and then lysed. The expression of PDGFR and BRD4 was analysed by western blot. Actin was processed in parallel as a loading control. Densitometric results are shown as means ± SD of three independent experiments.

6) Summary

While the antiproliferative effect of Sulforaphane and JQ1 on VSMC have already been reported, the combination of these two compounds has not been studied in VSMC so far. In this diploma thesis the inhibitory effect of single and combinatorial treatment with Sulforaphane and JQ1 on VSMC proliferation was investigated. Sulforaphane and JQ1 both inhibited VSMC proliferation concentration-dependently and arrested the cell cycle at the G1 phase, which is in line with previous investigations. The combinatorial treatment showed an antagonistic effect with regards to VSMC proliferation. Interestingly, Sulforaphane and JQ1 did not antagonize, but enhance the expression of the NRF2-dependent enzymes GCLC and HO-1 in an additive or synergistic fashion. This data set presumably indicates that Nrf2 target gene expression does not play an essential role in VSMC proliferation. The BRD4 - as well as the PDGFR levels, were not altered much by SFN and JQ1 treatment.

These results may call for caution when intending to block VSMC proliferation in patients with restenosis with a combination of Sulforaphane and JQ1. Future studies are needed to fully understand the antagonistic effect of SFN and JQ1 in particular, and of Nrf2 activation and BET inhibition in general, with respect to proliferation of activated VSMC.

D) Abbreviations

A

Ac-H3	Acetyl Histone 3
ALL	Acute lymphoblastic leukemia
AML	Acute myeloid leukemia
AngII	Angiotensin II
APS	Ammonium peroxodisulfate
ARE	Antioxidant response element
ASMC	Aortic smooth muscle cells

B

BD	Bromodomain
BET	Bromo and extraterminal domain
BRD4	Bromodomain-containing protein 4
BSA	Bovine serum albumin
β-TrCP	Beta-transducin repeat containing E3 ubiquitin protein ligase

C

CDDO-IM	1-(2-cyano-3,12-dioxooleana-1,9-dien-28-oyl) imidazole
CI	Combinatorial index
CncC	Cap 'n'collar isoform C
CO_2	Carbon dioxide
CONC	Concentration
COPD	Chronic obstructive pulmonary disease
Cul-3	Cullin3

D

DMEM	Dulbecco's Modified Eagle's Medium
DMSO	Dimethyl sulfoxide
DNMT	DNA methyl-transferases

E

EDTA	Ethylenediaminetetraacetic acid
ERK	Extracellular signal–regulated kinases
Et al.	Et alii (and others)
ETOH	Ethanol

F

FACS	Fluorescence - activated cell sorting
FBS	Fetal Bovine Serum
Fs(1)h	Female sterile homeotic

G

GCLC	Glutamate—cysteine ligase catalytic subunit
GM	Growth medium
GSK3b	Glycogen synthase kinase 3 beta

H

HAT	Histone acetyl-transferase
HDAC	Histone deacetylases
HO-1	Heme oxygenase 1
HRP	Horseradish peroxidase

I

IC50	Half maximal inhibitory concentration
i.e.	id est (that is to say)
IgG	Immunoglobulin G
IL	Interleukin
IRES	Internal ribosomal entry side

K

Keap1	Kelch-like ECH-associated protein 1

L

Ltd.	Limited

M

MAPK	Mitogen-activated protein kinase
MEK1/2	Mitogen-activated protein kinase kinase
MM	Multiple myeloma
MRP2	Multidrug resistance-associated protein 2
mRNA	Messenger Ribonucleic acid
mTOR	Mechanistic Target of Rapamycin

N

N.a.	Not applicable
NaOH	Sodium hydroxide
NEH1	Nrf2-ECH-homology 1
NEH2	NRF2-ECH homology–like domain 2
NF-κB	Nuclear factor kappa B
NO	Nitrogen monoxide
NQO1	NAD(P)H dehydrogenase [quinone] 1
NRF2	Nuclear factor erythroid 2-related factor 2

O

OD	Optical density
oxLDL	Oxidized LDL

P

P-TEFb	Positive transcription elongation factor
PAA	Phenylacetic acid
PBS	Phosphate buffered saline
PDGF	Platelet derived growth factor
PI	Propidium iodide
PMSF	Phenylmethanesulphonylfluoride

R

RBS	rRNA binding site
Rbx1	RING-box protein 1
RIPA	Radioimmunoprecipitation assay
ROS	Reactive oxygen secies
Rpm	Rotations per minute
RT	Room temperature

S

SD	Standard deviation
SDS-PAGE	Sodium dodecyl sulfate polyacrylamide gel electrophoresis
Ser	Serine
SFN	Sulforaphane
SQSTM1	Sequestosome-1
ST	Starvation medium

T

TAF7	Transcription initiation factor TFIID subunit 7
TBST	Tris-buffered saline with Tween20
TEMED	Tetramethylethylendiamin
TNF-α	Tumor necrosis factor alpha

V

VSMC	Vascular smooth muscle cells

E) References

Alexander, M.R., Owens, G.K. (2012) Epigenetic control of smooth muscle cell differentiation and phenotypic switching in vascular development and disease. Annu Rev Physiol. 74, 13–40.

Arshad Z., Smith J., Roberts M., Lee W. H., Davies B., Bure K., et al. . (2016) Open access could transform drug discovery: a case study of JQ1. Expert Opin. Drug Discov. 11, 321–332.

Ashino T., Yamamoto M., Yoshida T., Numazawa S. (2013) Redox-sensitive transcription factor Nrf2 regulates vascular smooth muscle cell migration and neointimal hyperplasia. Arterioscler Thromb Vasc Biol. 33, 760–768.

Bai, Y., Wang, X., Zhao, S., Ma, C., Cui, J., & Zheng, Y. (2015) Sulforaphane Protects against Cardiovascular Disease via Nrf2 Activation. Oxidative medicine and cellular longevity. 2015, 407580.

Chatterjee, N. and Bohmann, D. (2018) BET-ting on Nrf2: How Nrf2 Signaling can Influence the Therapeutic Activities of BET Protein Inhibitors. BioEssays. 40(5), 1800007.

Chatterjee, N., Tian, M., Spirohn, K., Boutros, M., & Bohmann, D. (2016) Keap1-Independent Regulation of Nrf2 Activity by Protein Acetylation and a BET Bromodomain Protein. PLoS genetics. 12(5), e1006072.

Cho, S., Hazama, M., Urata, Y., Goto, S., Horiuchi, S., Sumikawa, K., Kondo, T. (1999) Protective role of glutathione synthesis in response to oxidized low density lipoprotein in human vascular endothelial cells. Free Radic Biol Med. 26, 589-602.

Das, S., Senapati, P., Chen, Z., Reddy, M. A., Ganguly, R., Lanting, L., Mandi, V., Bansal, A., Leung, A., Zhang, S., Jia, Y., Wu, X., Schones, D. E., … Natarajan, R. (2017) Regulation of angiotensin II actions by enhancers and super-enhancers in vascular smooth muscle cells. Nature communications. 8(1), 1467.

Di Costanzo, A., Del Gaudio, N., Migliaccio, A. Epigenetic drugs against cancer: an evolving landscape. (2014) Arch Toxicol. 88(9), 1651–1668.

Di Pietro, M., Filardo, S., Falasca, F., Turriziani, O., & Sessa, R. (2017) Infectious Agents in Atherosclerotic Cardiovascular Diseases through Oxidative Stress. International journal of molecular sciences. 18(11), 2459.

Eggler, A. L., Small, E., Hannink, M., & Mesecar, A. D. (2009) Cul3-mediated Nrf2 ubiquitination and antioxidant response element (ARE) activation are dependent on the partial molar volume at position 151 of Keap1. The Biochemical journal. 422(1), 171-80.

Feoktistova, M., Geserick, P., Leverkus, M. (2016) Crystal Violet Assay for Determining Viability of Cultured Cells. Cold Spring Harb Protoc. 2016(4).

Ferri E., Petosa C., McKenna C.E. (2016) Bromodomains: Structure, function and pharmacology of inhibition. Biochem Pharm. 106,1–18.

Guo, Y., Yu, S., Zhang, C., & Kong, A. N. (2015) Epigenetic regulation of Keap1-Nrf2 signaling. Free radical biology & medicine. 88(Pt B), 337-349.

Hu, C., Eggler, A. L., Mesecar, A. D., & van Breemen, R. B. (2011) Modification of keap1 cysteine residues by sulforaphane. Chemical research in toxicology. 24(4), 515-21.

Huang, Y., Li, W., Su, Z. Y., & Kong, A. N. (2015) The complexity of the Nrf2 pathway: beyond the antioxidant response. The Journal of nutritional biochemistry. 26(12), 1401-13.

Juan S. H., Lee T. S., Tseng K. W., et al. (2001) Adenovirus-mediated heme oxygenase-1 gene transfer inhibits the development of atherosclerosis in apolipoprotein E-deficient mice. *Circulation*. 104(13), 1519–1525.

Kawai, Y., Garduño, L., Theodore, M., Yang, J., & Arinze, I. J. (2010) Acetylation-deacetylation of the transcription factor Nrf2 (nuclear factor erythroid 2-related factor 2) regulates its transcriptional activity and nucleocytoplasmic localization. *The Journal of biological chemistry*. *286*(9), 7629-40.

Kensler, T. W., Egner, P. A., Agyeman, A. S., Visvanathan, K., Groopman, J. D., Chen, J. G., Chen, T. Y., Fahey, J. W., … Talalay, P. (2013) Keap1-nrf2 signaling: a target for cancer prevention by sulforaphane. Topics in current chemistry. 329, 163-77.

Kwon, J.S., Joung, H,. Kim, Y.S. et al. (2012) Sulforaphane inhibits restenosis by suppressing inflammation and the proliferation of vascular smooth muscle cells. Atherosclerosis. 225(1), 41–49.

Li, W., Thakor, N., Xu, E. Y., Huang, Y., Chen, C., Yu, R., Holcik, M., … Kong, A. N. (2009) An internal ribosomal entry site mediates redox-sensitive translation of Nrf2. Nucleic acids research. 38(3), 778-88.

Lydeard, J. R., Schulman, B. A., & Harper, J. W. (2013) Building and remodelling Cullin-RING E3 ubiquitin ligases. *EMBO reports*. *14*(12), 1050–1061.

Marx, S. O., Totary-Jain, H., & Marks, A. R. (2011) Vascular smooth muscle cell proliferation in restenosis. Circulation. Cardiovascular interventions. 4(1), 104-11.

Matzinger, M., Fischhuber, K., & Heiss, E. H. (2017) Activation of Nrf2 signaling by natural products-can it alleviate diabetes?. Biotechnology advances. 36(6), 1738-1767.

Michaeloudes, C., Mercado, N., Clarke, C., Bhavsar, P. K., Adcock, I. M., Barnes, P. J., & Chung, K. F. (2014) Bromodomain and extraterminal proteins suppress NF-E2-related factor 2-mediated antioxidant gene expression. Journal of immunology (Baltimore, Md. : 1950). 192(10), 4913-4920.

Mimura, J., Itoh, K. (2015) Role of Nrf2 in the pathogenesis of atherosclerosis. Free Radic Biol Med, 88 (Pt B), 221-232.

Noguchi-Yachide T. (2016) BET bromodomain as a target of epigenetic therapy. Chem Pharm Bull. 64(6), 540–547.

Ollinger, R., Bilban, M., Erat, A., Froio, A., McDaid, J., Tyagi, S., Csizmadia, E., Graca-Souza, A.V., Liloia, A., Soares, M.P., Otterbein, L.E., Usheva, A., Yamashita, K., Bach, F.H. (2005) Bilirubin: a natural inhibitor of vascular smooth muscle cell proliferation. *Circulation*. 112, 1030–1039.

Otterbein LE, Zuckerbraun BS, Haga M, Liu F, Song R, Usheva A, Stachulak C, Bodyak N, Smith RN, Csizmadia E, Tyagi S, Akamatsu Y, Flavell RJ, Billiar TR, Tzeng E, Bach FH, Choi AM, Soares MP. (2003). Carbon monoxide suppresses arteriosclerotic lesions associated with chronic graft rejection and with balloon injury. *Nat Med*. 9(2), 183–190.

Payen L., Courtois A., Loewert M., Guillouzo A., Fardel O. (2001) Reactive oxygen species-related induction of multidrug resistance-associated protein 2 expression in primary hepatocytes exposed to sulforaphane. Biochem Biophys Res Commun. 282(1), 257–263.

Perez, J., Hill, B. G., Benavides, G. A., Dranka, B. P., & Darley-Usmar, V. M. (2010) Role of cellular bioenergetics in smooth muscle cell proliferation induced by platelet-derived growth factor. *The Biochemical journal*. *428*(2), 255–267.

Picot, J., Guerin, C. L., Le Van Kim, C., & Boulanger, C. M. (2012) Flow cytometry: retrospective, fundamentals and recent instrumentation. *Cytotechnology*. *64*(2), 109–130.

Rada, P., Rojo, A. I., Evrard-Todeschi, N., Innamorato, N. G., Cotte, A., Jaworski, T., Tobón-Velasco, J. C., Devijver, H., García-Mayoral, M. F., Van Leuven, F., Hayes, J. D., Bertho, G., ... Cuadrado, A. (2012) Structural and functional characterization of Nrf2 degradation by the glycogen synthase kinase 3/β-TrCP axis. Molecular and cellular biology. 32(17), 3486-99.

Rajendran P., Johnson G., Li L., Chen YS., Dashwood M., Nguyen N., Ulusan A., Ertem F., Zhang M., Li J., Sund D., Huang Y., Wang S., Leung HC., ... Dashwood R. (2019) Acetylation of CCAR2 Establishes a BET/BRD9 Acetyl Switch in Responce to Combined Deacetylase and Bromodomain Inhibition. Cancer Res. 79(5), 918-927.

Shang, G., Tang, X., Gao, P., Guo, F., Liu, H., Zhao, Z., Chen, Q., Jiang, T., Zhang, N., & Li, H. (2015) Sulforaphane attenuation of experimental diabetic nephropathy involves GSK-3 beta/Fyn/Nrf2 signaling pathway. J Nutr Biochem. 26(6), 596–606.

Shawky, N. M., & Segar, L. (2017) Sulforaphane inhibits platelet-derived growth factor-induced vascular smooth muscle cell proliferation by targeting mTOR/p70S6kinase signaling independent of Nrf2 activation. Pharmacological research. 119, 251-264.

Takaya, K., Suzuki, T., Motohashi, H., Onodera, K., Satomi, S., Kensler, T. W., & Yamamoto, M. (2012) Validation of the multiple sensor mechanism of the Keap1-Nrf2 system. Free radical biology & medicine. 53(4), 817-27.

Vaillancourt, M., Ruffenach, G., Meloche, J., Bonnet, S. (2015) Adaptation and remodelling of the pulmonary circulation in pulmonary hypertension. Can J Cardiol. 31(4), 407–415.

Wang, B., Zhang, M., Takayama, T., Shi, X., Roenneburg, D. A., Kent, K. C., & Guo, L. W. (2015) BET Bromodomain Blockade Mitigates Intimal Hyperplasia in Rat Carotid Arteries. EBioMedicine. 2(11), 1650-61.

Wang, D., Uhrin, P., Mocan, A., Waltenberger, B., Breuss, J.M., Tewari, D., Mihaly-Bison, J., Huminiecki, L., Starzyński, R., Tzvetkov, N.T., Horbańczuk, J., Atanasov, A.G. (2018) Vascular smooth muscle cell proliferation as a therapeutic target. Part 1. Biotechnol Adv. 36(6), 1586-1607.

White M.E., Fenger J.M., Carson W.E.. (2019) Emerging roles of and therapeutic strategies targeting Brd4 in cancer. Cell Immunol. 337, 48-53.

Yet, S.F., Layne, M.D., Liu, X., Chen, Y.H., Ith, B., Sibinga, N.E., Perrella, M.A. (2003) Absence of heme oxygenase-1 exacerbates atherosclerotic lesion formation and vascular remodeling. FASEB J. 17(12), 1759–1761.

Yoo, S.H., Lim, Y., Kim, S.J., Yoo, K.D., Yoo, H.S., Hong, J.T., Lee, M.Y., Yun, Y.P. (2013) Sulforaphane inhibits PDGF-induced proliferation of rat aortic vascular smooth muscle cell by up-regulation of p53 leading to G1/S cell cycle arrest. Vascular Pharmacol. 59(1-2),44–51.

Yu, R., Chen, C., Mo, Y-Y., Hebbar, V., Owuor, ED., Tan, T-H., Kong, A-NT. (2000) Activation of mitogen-activated protein kinase pathways induces antioxidant response element-mediated gene expression via a Nrf2-dependent mechanism. J Biol Chem. 275, 39907–39913.

Zhang, C., Su, Z. Y., Khor, T. O., Shu, L., & Kong, A. N. (2013) Sulforaphane enhances Nrf2 expression in prostate cancer TRAMP C1 cells through epigenetic regulation. Biochemical pharmacology. 85(9), 1398-404.

Zhang, D. D., & Hannink, M. (2003) Distinct cysteine residues in Keap1 are required for Keap1-dependent ubiquitination of Nrf2 and for stabilization of Nrf2 by chemopreventive agents and oxidative stress. Molecular and cellular biology. 23(22), 8137-51.

Zhang, HT., Gui, T., Sang, Y. et al. (2017). The BET bromodomain inhibitor JQ1 suppresses chondrosarcoma cell growth via regulation of YAP/p21/c-Myc signaling. J Cell Biochem. 118(8), 2182- 2192.

Zhu, H., Jia, Z., Zhang, L. et al. (2008) Antioxidants and phase 2 enzymes in macrophages: regulation by Nrf2 signaling and protection against oxidative and electrophilic stress. Experimental Biology and Medicine. 233(4), 463–474.

F) Acknowledgement

Elhamdulillahi Rabbil Alemin - All the praise belongs to Allah, the Almighty, the creator of the universes. He is the one who gave me existence and everything else I needed and he is the only source of my motivation. Therefore, I dedicate this work to his beloved one, prophet Muhammed (peace be upon him).

I would like to express my deepest gratitude to Prof. Dr. Elke Heiss, who not only enabled me to work within the "Molecular Targets" group, but also accompanied and supported me very kindly and patiently through my whole diploma thesis from the very beginning till the end.

At this point I would also like to thank the whole Molecular Targets Groups as I gained a lot of experience and also had a great time during my work.

My deepest gratitude goes to my mother Aysegül, my father Hasan and my elder sister Rümeysa, as well as to all my friends for always encouraging me in my life.